

Partially Observable Online Change Detection via Smooth-Sparse Decomposition

Jie Guo¹, Hao Yan², Chen Zhang^{1*}, Steven Hoi³

¹Tsinghua University

²Arizona State University

³Singapore Management University

Abstract

We consider online change detection of high dimensional data streams with sparse changes, where only a subset of data streams can be observed at each sensing time point due to limited sensing capacities. On the one hand, the detection scheme should be able to deal with partially observable data and meanwhile have efficient detection power for sparse changes. On the other, the scheme should be able to adaptively and actively select the most important variables to observe to maximize the detection power. To address these two points, in this paper, we propose a novel detection scheme called CDSSD. In particular, it describes the structure of high dimensional data with sparse changes by smooth-sparse decomposition, whose parameters can be learned via spike-slab variational Bayesian inference. Then the posterior Bayes factor, which incorporates the learned parameters and sparse change information, is formulated as a

*Corresponding author

detection statistic. Finally, by formulating the statistic as the reward of a combinatorial multi-armed bandit problem, an adaptive sampling strategy based on Thompson sampling is proposed. The efficacy and applicability of our method in practice are demonstrated with numerical studies and a real case study.

1 Introduction

High dimensional sequential change point detection has been extensively studied in statistics and machine learning. Sequential samples from p variables, $\mathbf{X}_1, \mathbf{X}_2, \dots$ are identically and independently distributed from a distribution in a dimensional space $\mathbf{X} \in \mathcal{R}^p$. The p variables of each sample may have complex correlations with each other, depending on the data structure of \mathbf{X}_t . For example, \mathbf{X}_t can be a vector, a profile, an image, etc. We aim at detecting a possible change point τ . Before it, the samples $\mathbf{X}_t, t \leq \tau$ follow a known distribution f_0 . After the change point, the samples \mathbf{X}_t follow another unknown post-change distribution f_1 . The goal is to detect the unknown change point as soon as possible after it occurs. We restrict our attention to detecting one change point, which often arises in sequential monitoring problems ([Montgomery 2007](#)).

For high dimensional data modeling, the correlation information of variables is hard to compute due to the curse of dimensionality. Consequently, dimension reduction methods, such as dictionary learning and matrix decomposition methods ([Cheng et al. 2018](#); [Qi et al. 2017](#)), are usually adopted to describe the high dimensional data in the feature level. Furthermore, when a change happens, it usually affects a few variables simultaneously. So we need to consider the variable correlation structure existing in the change as well. In other words, the dictionary should include both patterns of normal data and the patterns of the changed(abnormal) data. We further assume that when a change happens, it can be linearly represented by a few anomaly patterns in the dictionary([Mo et al. 2013](#)). Considering the dictionary is large, the linear representation would be sparse. This brings new demand for

more powerful detection schemes. Specifically, if we know that which potential abnormal patterns would affect which variables, then the corresponding detection scheme will only focus on these patterns and filter out background noise from other unchanged features.

Besides the challenges above, another emerging challenge in sequential change detection is limited sensing resources. Classical researches for high dimensional data sequential sparse change detection focus on a fully observable process, i.e., at each sampling time point, all the p variables in \mathbf{X}_t can be observed for analysis. However, in reality, sometimes it is unfeasible to acquire measurements of all these variables in real time. Instead, only a subset of the p variables can be accessible, such as in the following scenarios: (1) when the number of sensors cannot exceed certain number due the limited sensing resources; (2) when only a limited number of sensors can be set at "ON" mode due to limited battery lifetime; (3) when only partial data collected at each acquisition time can be transmitted back to fusion center for real-time analysis due to limited transmission bandwidth and computing speed. In any of the above-mentioned scenarios, only a subset of \mathbf{X}_t with m variables out of the p variables ($m \leq p$) can be observed. This further increases the difficulty of high dimensional sparse change detection. It requires us to not only deal with partial observations, but also develop a smart sensor allocation strategy to choose which variables to observe at each time point. Otherwise, if variables containing change patterns can not be observed, the change would never be detected.

In this paper, we aim at this problem of Partially Observable High Dimensional data Sequential Sparse Change Detection (POHDSSCD). Our goal is to develop a sequential detection algorithm for sparse changes, which can dynamically choose a subset of variables to observe at each time point such that the detection power can be maximized without violating the sensing constraints. In particular, (i) we describe the structure of high dimensional correlated data streams with sparse changes in feature level by smooth-sparse decomposition (SSD) (Yan et al. 2017). The decomposition, on one hand, can describe the data feature for before-change distribution f_0 , and on the other, can be customized to detect any specified

sparse change f_1 . (ii) Under the Bayesian learning framework with partial observations, we use the spike-slab variational Bayesian inference to learn the parameters of the decomposition, based on which a detection statistic is constructed by the posterior Bayes factor. (iii) Furthermore, we formulate the detection statistic as the reward function in the combinatorial multi-armed bandit problem and propose a Thompson sampling strategy to decide the most informative subset of variables to observe for the next sampling point such that the detection power can be maximized.

The remainder of the article is organized as follows. In Section 2, we review the literature of some related topics to the proposed problem. Section 3 describes more specific problem formulation. Section 4 introduces the main body of our proposed method sequentially, including variational Bayesian inference, Bayesian hypothesis testing and Thompson sampling. Section 5 presents a simulation study on synthetic data and a real-world case study to further illustrate the efficacy and effectiveness of the proposed method.

2 Related Works

To better describe the proposed framework, we would like to discuss some related state-of-the-art methods in the field of statistics and machine learning.

Sequential sparse change detection for multivariate streaming data has recently attracted increasing attention in many applications. Considering for the high dimensional data where only a sparse subset of variables may be affected by the change, many works utilized the idea of sparse learning for sparse change detection (Chan 2017; Wang and Mei 2013). For example, Wang and Jiang (2009) proposed a penalized likelihood function to screen out potential out-of-control variables. Similarly, Zou and Qiu (2009) adopted LASSO regularity to force sparse regularization on the estimated changes. Most of these methods assume the correlation matrix of different variables is known in advance or can be estimated via some historical data. Yet this is not true for the high-dimensional process due to the

curse of dimensionality. To solve it, one kind of method is to modify the estimation of the correlation matrix, by assuming it is diagonal (Mei 2010). Then univariate detection statistics for each dimension are constructed separately, but only statistics of the top R most likely changed variables are fused together as the final statistic to filter out noises (Mei 2010). However, this loss of correlation information compromises the detection power a lot. Another kind of method is to use dimension reduction or a low-rank approximation to describe the correlation structure. In particular, Zhang et al. (2018) proposed a sparse functional principal component analysis (PCA) to model multi-channel profiles. Then the sparse PCA scores are used to construct a detection statistic for online monitoring multi-channel profile data. Yan et al. (2017) described the high dimensional spatial correlation in image data by smooth-sparse decomposition. Then the sparse anomalous regions are learned and the LASSO based detection statistic of Zou and Qiu (2009) is constructed. However, all these methods can only be applied in fully observable scenarios, therefore do not apply for partially observed data.

Partial observable sequential change detection is an emerging topic that has not been fully addressed. The most pioneer work Liu et al. (2015) proposed a top- R detection scheme by extending Mei (2010) to the scenario with missing observation. Later Xian et al. (2017) extended the work of Liu et al. (2015) to non-Gaussian process, by constructing an anti-rank detection statistic based on data spatial structure. However, these two methods treat different variables as independent without exploiting their correlation structure. This leads to their methods perform poorly in some scenarios, as shown in Section 5. On the one hand, taking advantage of the correlation structure can improve the detection efficiency, especially when the change influences some sensors jointly. On the other hand, if a variable is not observed, its information can still be inferred based on its correlation with other observed variables. Later Wang et al. (2018a) proposed a spatial-adaptive sampling and monitoring procedure that utilized the spatial information of the data streams for quick change detection. Xian et al. (2019) revised the rank-based statistic of Xian et al. (2017) by containing

the correlation information. It can automatically augment information for unobservable variables based on other observed ones, and intelligently allocate the monitoring resources to the most suspicious data streams. However, all these adaptive sampling strategies are heuristic, and their adaptive sampling strategies are based on rule of thumb without any theoretical guarantee. Recently, [Zhang and Hoi \(2019\)](#) exploited the relationship between partial observable online detection with a combinatorial multi-armed bandit, and proposed an adaptive sampling strategy based on the upper confidence bound (UCB) algorithm. This work also analyzed the theoretical property of lower bound of detection power. However, it has the limitation of huge computation complexity and is unpractical to be applied in the high dimensional process. In addition, to deal with the correlation of variables, all existing methods assume the covariance matrix is known and directly use it to formulate the monitoring statistic. As mentioned earlier, this cannot be satisfied in reality. Furthermore, these methods do not target at sparse change, and consequently have limited power for the POHDSSCD problem.

Multi-armed bandit (MAB) is a problem extensively studied in reinforcement learning and online learning. It considers a system with p arms where in each round one arm (or a combinatorial subset of arms) can be selected and a reward is achieved. The reward of each arm (or each combinatorial set) follows a certain distribution with unknown expectation, and the objective of MAB (or combinatorial MAB, i.e., CMAB) is to play these arms in sequential rounds with an arm selection policy such that the total expected reward can be maximized. In our scenario, we want to sequentially decide the best subset of variables so as to minimize the average detection delay, which is similar to the objective of CMAB. Hence we can borrow some ideas from MAB related works. So far, a number of studies have been done on developing sampling strategies for MAB problems. In general, they can be classified into two categories: the UCB ([Chen et al. 2013](#)) and the Thompson sampling algorithms ([Durand and Gagné 2014](#)). Built upon them, some works also have studied how to choose the best top- K arms ([Even-Dar et al. 2006](#); [Bubeck et al. 2013](#)), or the outlier arms ([Zhuang et al.](#)

2017). However, these methods assume the system is static, i.e., the reward distribution of arms do not change sequentially. Yet our problem is more about identifying the change of the system. Furthermore, they target at single or top- K arms (or variables) identification. Yet in our problem, we would like focus on system level detection. Recently, there are also some works combining change point detection algorithms with bandit algorithms. Considering that the reward of each arm is not stationary but piecewise-constant and the shifts at unknown time points are change points, Liu et al. (2018); Cao et al. (2019) combined change point detection procedures with UCB method, to track the time-varying reward distributions. Yet their objective is still maximizing the total expected reward, instead of system change detection.

3 Problem Formulation

Consider a system consisting of p variables. Denote the signals of these variables at sensing time point t as $\mathbf{X}_t = (X_{1t}, \dots, X_{pt})$. We assume in the normal condition $\mathbf{X}_t \stackrel{iid}{\sim} f_0$ for $t = 1, 2, \dots$, and we are interested in detecting any change of these p variables. For high-dimensional \mathbf{X}_t , dictionary learning and representation is commonly used to reduce dimension and describe the complex correlation structure of data (Cheng et al. 2018; Qi et al. 2017). Following their general decomposition formulation, we assume for normal \mathbf{X}_t , it can be expanded on a before-change feature space with k_b bases $\mathbf{B}_b = [\mathbf{b}_{b1}, \dots, \mathbf{b}_{bk_b}] \in \mathcal{R}^{p \times k_b}$, i.e.,

$$\mathbf{X}_t = \mathbf{B}_b \boldsymbol{\theta}_t + \mathbf{E}_t, \tag{1}$$

where $\boldsymbol{\theta}_t \in \mathcal{R}^{k_b \times 1}$ are the coefficients and $\mathbf{E}_t \in \mathcal{R}^{p \times 1}$ are the noise terms. In this paper, we assume \mathbf{E}_t follows a Gaussian distribution as $\mathbf{E}_t \sim N(\mathbf{0}, \boldsymbol{\Sigma}_e)$ with $\boldsymbol{\Sigma}_e = \sigma_e^2 \mathbf{I}$. Here \mathbf{B}_b can be either learned by historical observed samples via matrix decomposition algorithms,

or be set as notable spaces such as Spline space (Meier et al. 2009), Fourier space, Kernel space, etc (Wang et al. 2018b). Consequently, the decomposition can explain the data covariance matrix as $\text{Cov}(\mathbf{X}_t) = \mathbf{B}_b \text{Cov}(\boldsymbol{\theta}_t) \mathbf{B}_b' + \boldsymbol{\Sigma}_e$. Since the rank of $\text{Cov}(\boldsymbol{\theta}_t)$ is generally much smaller than that of \mathbf{X}_t , this is exactly the low rank estimation for high-dimensional covariance matrix (Fan et al. 2008; Cai et al. 2016). In this paper, without loss of generality, we further assume the projection of \mathbf{X}_t on the before-change bases is stable and $\boldsymbol{\theta}_t$ follows a Gaussian distribution with mean $\mathbf{0}$ and covariance matrix $\boldsymbol{\Sigma}_0$. Then we can have $\text{Cov}(\mathbf{X}_t) = \mathbf{B}_b \boldsymbol{\Sigma}_0 \mathbf{B}_b' + \boldsymbol{\Sigma}_e$.

When \mathbf{X}_t occurs sparse changes, unlike the before-change distribution of f_0 focusing on low-rank structures, many types of sparse changes with diverse anomaly patterns may occur in the system, and the chance that each type of anomaly pattern happens is pretty small. With this in mind, we may further define an anomaly dictionary with a set of anomaly bases $\mathbf{B}_a = [\mathbf{b}_{a1}, \dots, \mathbf{b}_{ak_a}]$. Here k_a can be even larger than p . \mathbf{B}_a can either be set by domain knowledge from practitioners, if certain specific change patterns are of interest, or be learned from some collected anomaly data via the dictionary learning approach. In conclusion, we can utilize a composite decomposition approach to describe the post-change distribution f_1 with sparse change patterns from f_0 , i.e.,

$$\mathbf{X}_t = \mathbf{B}_b \boldsymbol{\theta}_t + \mathbf{B}_a \boldsymbol{\theta}_a + \mathbf{E}_t. \quad \forall t > \tau \quad (2)$$

In this paper, considering that in most of the applications, the anomaly bases generally have components outside the subspace spanned by the normal bases (Xu et al. 2020; Zhang and Zhang 2018), we further assume that $\mathbf{B}_b' \mathbf{B}_a = \mathbf{0}$.

This concept of composite decomposition can be dated back to additive models (Wood et al. 2015), where a nonparametric regression is defined as a combination of several composite models. Later similar concepts have been applied in many applications. Ba et al. (2012) proposed a ‘‘composite Gaussian process’’ to describe global features and local features of

expensive functions. Zhang et al. (2016) constructed an additive Gaussian process model with two separate Gaussian processes to describe characteristics of desired profile and abnormal profile data. Yan et al. (2017) decomposed image signal into a smooth functional mean plus sparse anomalous regions, for image anomaly detection.

Combining (1) and (2), we can define the change-point model as this: $\boldsymbol{\theta}_a = \mathbf{0}, \forall t \leq \tau$, and $\boldsymbol{\theta}_a \neq \mathbf{0}, \forall t > \tau$. In real online change detection scenario, since τ is unknown, our goal is to construct a hypothesis test to decide whether

$$H_0 : \boldsymbol{\theta}_a = \mathbf{0}, \quad H_1 : \boldsymbol{\theta}_a \neq \mathbf{0}, \quad (3)$$

for each time point t , based on the partially observed subset of \mathbf{X}_t . Here we introduce a sensing variable z_{it} for each variable X_{it} such that $z_{it} = 1$ if and only if X_{it} is observed at time point t , and the sensing constraint can be expressed as $\sum_{i=1}^p z_{it} = m, \forall t$. Denote $Z(t)$ to be the vector of indices corresponding to the observed dimensions for \mathbf{X}_t . $\mathbf{X}_{Z(t)} \in \mathcal{R}^{m \times 1}$ represents the observed data for time point t .

We would like to construct a detection scheme for (3). We assume that after τ , the change would keep. We construct the scheme relating to a stopping time T associated with a test statistic $\Lambda(t)$. The scheme defines a stopping time $T = \inf_t \{\Lambda(t) > h\}$ where h is a pre-defined constant threshold, and $T = n$ is explained as the detection scheme stops at time n and indicates that there exists a change among the first n time points. The performance of the detection scheme can be evaluated by two criteria: Average Run Length (ARL), before a false alarm occurs in normal condition, i.e., $ARL_0 = E(T | \tau = \infty)$, and Average Detection Delay (ADD) after a change occurs in abnormal condition, i.e., $ADD_\tau = E(T - \tau | T > \tau, \tau < \infty)$. In practice, conditional on ARL as a fixed number which controls the false alarm rate, a detection scheme is formulated to minimize ADD.

4 Our Method

In this section, we propose a change detection scheme for POHDSSCD in the Bayesian framework. In particular, we construct an online variational Bayesian inference to estimate the posterior distribution of both $\boldsymbol{\theta}_t$ and $\boldsymbol{\theta}_a$ with sequential samples $\mathbf{X}_{Z(t)}$. The online estimation can make the best use of historical data and detect the nonzero $\boldsymbol{\theta}_a$ efficiently. Then the posterior distributions of $\boldsymbol{\theta}_t$ and $\boldsymbol{\theta}_a$ are used to construct a detection statistic for (3) based on posterior Bayes factor. The test statistic can be treated as the reward distribution of a CMAB problem, and accordingly, a Thompson sampling framework to maximize the reward is proposed for selecting observations for the next time point.

4.1 Spike-Slab Model

With the prior information that $\boldsymbol{\theta}_a$ is a sparse vector, we consider the prior distribution that each component of $\boldsymbol{\theta}_a$ follows a spike-slab model independently. The spike-slab prior has been commonly used in many models for sparse vector estimation (Mitchell and Beauchamp 1988). In particular, binary variables $\mathbf{r} = [r_1, \dots, r_{k_a}]$ are introduced to indicate whether θ_{aj} is nonzero. r_j is a Bernoulli random trial governed by common success rate $p(r_j = 1) = w_j$. If $r_j = 0$, $p_0(\theta_{aj})$ follows the Gaussian distribution with zero mean and variance $v\sigma_j^2$, with $v \ll 1$, e.g., the “spike”, which demonstrates that the probability $p_0(\theta_{aj}) = 0$ almost equals 1. Otherwise, $p_0(\theta_{aj})$ follows the Gaussian distribution with zero mean and variance σ_j^2 , e.g., the “slab”, which demonstrates that the probability $p_0(\theta_{aj} \neq 0)$ is large. This hierarchical prior distribution of $\boldsymbol{\theta}_a$ can be written as

$$\begin{aligned} p_0(\theta_{aj}|r_j, \sigma_j^2) &\sim N(0, r_j\sigma_j^2 + (1 - r_j)v\sigma_j^2), \\ p_0(r_j) &\sim \text{Bernoulli}(w_j), \quad j = 1, \dots, k_a. \end{aligned} \tag{4}$$

Based on (4), supposing the current time is n , we aim to estimate the posterior probability of $\boldsymbol{\theta}_a$ based on all the previous n samples $\mathbf{X}_{Z(t)}, t = 1, \dots, n$. Consider that samples in recent time points are more likely to represent the current system state and can better detect the changes of the current system state than samples in the past time points. We would like to impose more weights on the current time points in the estimation. As such, we enforce time decayed weights $\lambda_t^n, t = 1, \dots, n$ on the n samples, in the sense that $\lambda_1^n < \lambda_2^n \dots < \lambda_n^n$, and get the weighted posterior distribution of $\boldsymbol{\theta}_a$ as

$$p(\boldsymbol{\theta}_a, \mathbf{r} | \mathbf{X}_{Z(1)}, \dots, \mathbf{X}_{Z(n)}) \propto p_0(\boldsymbol{\theta}_a, \mathbf{r}) \prod_{t=1}^n p(\mathbf{X}_{Z(t)} | \boldsymbol{\theta}_a, \mathbf{r})^{\lambda_t^n}. \quad (5)$$

In this paper, we use the exponential decayed weights, i.e., $\lambda_t^n = \frac{\lambda(1-\lambda)^{n-t}}{1-(1-\lambda)^n}$ with a small positive value $\lambda \in (0, 0.1]$.

With the spike-slab model structure, we can reformulate our hypothesis of (3) as

$$H_0 : \boldsymbol{\theta}_a = \mathbf{0}, \quad H_1 : \boldsymbol{\theta}_a \sim N(\boldsymbol{\mu}_r, \mathbf{K}), \quad (6)$$

where $\boldsymbol{\mu}_r = \boldsymbol{\mu}_a \circ \mathbf{r}$, with \circ representing the element-wise product. $\boldsymbol{\mu}_a = [\mu_1, \dots, \mu_{k_a}]'$ is the estimated abnormal mean of the slab distribution of $\boldsymbol{\theta}_a$ and $\mathbf{K} = \text{diag} \left(((1-r_1)v + r_1)s_1^2, ((1-r_2)v + r_2)s_2^2, \dots, ((1-r_{k_a})v + r_{k_a})s_{k_a}^2 \right)$ is the estimated covariance matrix of $\boldsymbol{\theta}_a$.

4.2 Variational Bayesian Inference

Unfortunately, (5) does not have a closed-form solution. So here we propose to approximately estimate (5) using variational methods, which have been popularly adopted in the literature. Variational methods can achieve high efficiency in computing the posterior distributions when the number of parameters to be estimate is relatively large (Attias 2000; Carbonetto et al. 2012). Here, the idea of variational Bayesian approach is to approximate (5) via another distribution $q(\boldsymbol{\theta}_a, \mathbf{r}) = \prod_{j=1}^{k_a} q_j(\theta_{aj}, r_j)$, such that its Kullback-Leibler diver-

gence from the true posterior distribution (5) is minimized. This can be done by iteratively updating each $q_j(\theta_{aj}, r_j)$ sequentially with other $q_k(\theta_{ak}, r_k), k \neq j$ fixed until convergence. Following Carbonetto et al. (2012), we restrict $q_j(\theta_{aj}, r_j)$ to still have the form

$$\begin{aligned} q_j(\theta_{aj}|r_j) &\sim N(\theta_{aj}|r_j\mu_{aj}, r_js_j^2 + (1-r_j)vs_j^2), \\ q_j(r_j) &\sim \text{Bernoulli}(\alpha_j). \end{aligned} \quad (7)$$

Finding the best fully-factorized distribution $q_j(\theta_{aj}, r_j) = q_j(\theta_{aj}|r_j)q_j(r_j)$ indicates to find $\{\mu_{aj}, s_j^2, \alpha_j\}$ that minimize the Kullback-Leibler divergence. This is equivalent to maximizing the negative Kullback-Leibler divergence

$$\begin{aligned} Z &= \int q(\boldsymbol{\theta}_a, \mathbf{r}) \ln \frac{p(\boldsymbol{\theta}_a, \mathbf{r}, \mathbf{X}_{Z(1)}, \dots, \mathbf{X}_{Z(n)})}{q(\boldsymbol{\theta}_a, \mathbf{r})} dq(\boldsymbol{\theta}_a, \mathbf{r}) \\ &= E_{q(\boldsymbol{\theta}_a, \mathbf{r})}[\ln p(\boldsymbol{\theta}_a, \mathbf{r}, \mathbf{X}_{Z(1)}, \dots, \mathbf{X}_{Z(n)})] - E_{q(\boldsymbol{\theta}_a, \mathbf{r})}[\ln q(\boldsymbol{\theta}_a, \mathbf{r})]. \end{aligned} \quad (8)$$

The coordinate descent updates for this optimization problem can be obtained by taking the partial derivatives of the negative Kullback-Leibler divergence, setting the partial derivatives to zero, and solving for the parameter μ_{aj}, s_j^2 , and α_j . This yields coordinate updates:

$$\mu_{aj} = \frac{s_j^2}{\sigma_e^2} \times \left(\sum_{t=1}^n \lambda_t^n ((\mathbf{X}_{Z(t)} - \mathbf{B}_b \tilde{\boldsymbol{\theta}}_n)' \mathbf{B}_{ajZ(t)} + \sum_{k \neq j} \mathbf{B}'_{ajZ(t)} \mathbf{B}_{akZ(t)} \alpha_k \mu_{ak}) \right), \quad (9)$$

$$(s_j^2)^{-1} = \sum_{t=1}^n \frac{\lambda_t^n \mathbf{B}'_{ajZ(t)} \mathbf{B}_{ajZ(t)}}{\sigma_e^2} + \frac{1}{\sigma_j^2}, \quad (10)$$

$$\ln \frac{\alpha_j}{1 - \alpha_j} = \ln \frac{w_j}{1 - w_j} + \frac{\mu_{aj}^2}{2\sigma_j^2} + \sum_{t=1}^n \frac{\lambda_t^n}{2\sigma_e^2} \mathbf{B}'_{ajZ(t)} \mathbf{B}_{ajZ(t)} (\mu_{aj}^2 - s_j^2 + vs_j^2). \quad (11)$$

The deviation details are in Appendix A. Thus we set the posterior distribution of $\boldsymbol{\theta}_a$ as $\tilde{p}(\boldsymbol{\theta}_a|\mathbf{r}) = q(\boldsymbol{\theta}_a|\mathbf{r})$ and $\tilde{p}(\mathbf{r}) = q(\mathbf{r})$.

Based on $\tilde{p}(\boldsymbol{\theta}_a|\mathbf{r})$ and $\tilde{p}(\mathbf{r})$, we further update the posterior distribution of $\boldsymbol{\theta}_n$. Since we assume $\boldsymbol{\theta}_n$ is identically and independently distributed for different n , the likelihood function

$p((\mathbf{X}_n - \mathbf{B}_a \boldsymbol{\theta}_a) | \boldsymbol{\theta}_n)$ is only related to the current observation \mathbf{X}_n . Assume its prior also follows a Gaussian distribution $p_0(\boldsymbol{\theta}_n) \sim N(\mathbf{0}, \boldsymbol{\Sigma}_b)$ with $\boldsymbol{\Sigma}_b = \sigma_b^2 \mathbf{I}$. According to Bayesian updating rule, the posterior distribution of $\boldsymbol{\theta}_n$ still follows a multivariate Gaussian distribution as $\tilde{p}(\boldsymbol{\theta}_n) \sim N(\tilde{\boldsymbol{\theta}}_n, \tilde{\boldsymbol{\Sigma}}_b)$ with

$$\tilde{\boldsymbol{\theta}}_n = (\mathbf{B}'_{bZ(n)} \boldsymbol{\Sigma}_e^{-1} \mathbf{B}_{bZ(n)} + \boldsymbol{\Sigma}_b^{-1})^{-1} \mathbf{B}'_{bZ(n)} \boldsymbol{\Sigma}_e^{-1} (\mathbf{X}_{Z(n)} - \mathbf{B}_{aZ(n)} \tilde{\boldsymbol{\mu}}_a), \quad (12)$$

$$\tilde{\boldsymbol{\Sigma}}_b = (\mathbf{B}'_{bZ(n)} \boldsymbol{\Sigma}_e^{-1} \mathbf{B}_{bZ(n)} + \boldsymbol{\Sigma}_b^{-1})^{-1}. \quad (13)$$

Here $\boldsymbol{\alpha} = [\alpha_1, \dots, \alpha_{k_a}]'$ and $\tilde{\boldsymbol{\mu}}_a = \boldsymbol{\mu}_a \circ \boldsymbol{\alpha}$.

By iteratively estimating $\{\boldsymbol{\mu}_a, \mathbf{s}^2, \boldsymbol{\alpha}\}$ and $\{\tilde{\boldsymbol{\theta}}_n, \tilde{\boldsymbol{\Sigma}}_b\}$ until convergence, we can get $\tilde{p}(\boldsymbol{\theta}_a, \mathbf{r})$ and $\tilde{p}(\boldsymbol{\theta}_n)$. The details of the estimation procedure are shown in Algorithm 1.

Algorithm 1: Variational Bayesian for $\boldsymbol{\theta}_a$ and $\boldsymbol{\theta}_n$

Input: Data $\mathbf{X}_t, t = 1, \dots, n, \boldsymbol{\theta}_t, t = 1, \dots, n - 1$

Initialize $\tilde{\boldsymbol{\theta}}_n = (\mathbf{B}'_{bZ(n)} \boldsymbol{\Sigma}_e^{-1} \mathbf{B}_{bZ(n)} + \boldsymbol{\Sigma}_b^{-1})^{-1} \mathbf{B}'_{bZ(n)} \boldsymbol{\Sigma}_e^{-1} \mathbf{X}_{Z(n)}$

$\tilde{\boldsymbol{\Sigma}}_b = (\mathbf{B}'_{bZ(n)} \boldsymbol{\Sigma}_e^{-1} \mathbf{B}_{bZ(n)} + \boldsymbol{\Sigma}_b^{-1})^{-1}$

repeat

for $j = 1, \dots, k_a$ **do**

 Update μ_{aj}, s_j^2 , and α_j via (9), (10) and (11).

 Update $\tilde{\boldsymbol{\theta}}_n$ and $\tilde{\boldsymbol{\Sigma}}_b$ via (12) and (13).

until *Converge*;

return $\boldsymbol{\mu}_a, \mathbf{s}^2, \boldsymbol{\alpha}, \tilde{\boldsymbol{\theta}}_n, \tilde{\boldsymbol{\Sigma}}_b$

4.3 Bayesian Hypothesis Testing

As an alternative to classic hypothesis testing to provide evidence to support a model over another (Kass and Raftery 1995), Bayes factor uses the likelihood ratio to quantify the evidence for hypothesis H_1 relative to hypothesis H_0 , i.e., $BF = \frac{\int L_1(\phi_1) \pi_1(\phi_1) d\phi_1}{\int L_0(\phi_0) \pi_0(\phi_0) d\phi_0}$, where $\phi_1 = \{\boldsymbol{\theta}_a, \boldsymbol{\theta}_n\}$, $\phi_0 = \{\boldsymbol{\theta}_n\}$, $\pi_i, i = 1, 0$ are the prior distributions and $L_j, j = 1, 0$ are the likelihood functions of the observations $\mathbf{X}_{Z(n)}$ under H_1 and H_0 . It has been extensively used in model selection (Morey and Rouder 2011; Wasserman 2000). However, one limitation of BF is

its sensitivity to variations in the prior, which may result in Lindley paradox in hypothesis testing (Aitkin 1991). Later, as an possible solution, Posterior BF is proposed by Aitkin (1991). It is defined as $PBF = \frac{p(\mathbf{X}_{Z(n)}|H_1)}{p(\mathbf{X}_{Z(n)}|H_0)} = \frac{\int L_1(\phi_1)\pi_1(\phi_1|\mathbf{X}_{Z(n)})d\phi_1}{\int L_0(\phi_0)\pi_0(\phi_0|\mathbf{X}_{Z(n)})d\phi_0}$, where $\pi_i(\phi_i|\mathbf{X}_{Z(n)})$, $i = 1, 0$ are the posterior distributions under H_1 and H_0 . PBF reflects the analyst's belief about the relative weighting of two competing hypotheses.

Here we construct the posterior Bayes factor based on the posterior of $\{\boldsymbol{\mu}_a, \mathbf{s}^2, \boldsymbol{\alpha}, \tilde{\boldsymbol{\theta}}_n, \tilde{\boldsymbol{\Sigma}}_b\}$ as detection statistic to decide whether $\boldsymbol{\theta}_a = \mathbf{0}$. By averaging over the uncertainty of parameters, we can compute the marginal probability of the data under the two competing hypotheses, i.e.,

$$p(\mathbf{X}_{Z(n)}|H_1) = \sum_{\mathbf{r} \in \mathcal{R}} \tilde{p}(\mathbf{r}) \iint \tilde{p}(\boldsymbol{\theta}_a|\mathbf{r})\tilde{p}(\boldsymbol{\theta}_n|\boldsymbol{\theta}_a)p(\mathbf{X}_{Z(n)}|\boldsymbol{\theta}_a, \boldsymbol{\theta}_n)d\boldsymbol{\theta}_nd\boldsymbol{\theta}_a, \quad (14)$$

$$p(\mathbf{X}_{Z(n)}|H_0) = \int \tilde{p}(\boldsymbol{\theta}_n|H_0)p(\mathbf{X}_{Z(n)}|\boldsymbol{\theta}_n)d\boldsymbol{\theta}_n. \quad (15)$$

where \mathcal{R} is the set of all possible values of \mathbf{r} . Then we will derive analytical forms for (14) and (15) in the following proposition.

Proposition 1. *The marginal likelihood can be estimated by integrating out the posterior distributions of the internal parameters $\{\boldsymbol{\theta}_a, \boldsymbol{\theta}_n\}$ as*

$$p(\mathbf{X}_{Z(n)}|H_0) = C_1 \exp\left(-\frac{1}{2}(\tilde{\boldsymbol{\theta}}_n^{[0]'}\tilde{\boldsymbol{\Sigma}}_b^{-1}\tilde{\boldsymbol{\theta}}_n^{[0]} + \mathbf{X}'_{Z(n)}\boldsymbol{\Sigma}_0^{-1}\mathbf{X}_{Z(n)} - \mathbf{G}^{[0]}\mathbf{H}^{-1}\mathbf{G}^{[0]'})\right), \quad (16)$$

and

$$p(\mathbf{X}_{Z(n)}|H_1) = C_2 \sum_{\mathbf{r} \in \mathcal{R}} p(\mathbf{r}|H_1) \exp\left(-\frac{1}{2}(\boldsymbol{\mu}'_r\mathbf{K}^{-1}\boldsymbol{\mu}_r + \mathbf{X}'_{Z(n)}\boldsymbol{\Sigma}_0^{-1}\mathbf{X}_{Z(n)} + \tilde{\boldsymbol{\theta}}_n^{[1]'}\tilde{\boldsymbol{\Sigma}}_b^{-1}\tilde{\boldsymbol{\theta}}_n^{[1]} - \mathbf{DA}^{-1}\mathbf{D}' - (\mathbf{G}^{[1]} - \mathbf{DA}^{-1}\mathbf{C}')(\mathbf{H} - \mathbf{CA}^{-1}\mathbf{C}')^{-1}(\mathbf{G}^{[1]} - \mathbf{DA}^{-1}\mathbf{C}')')\right). \quad (17)$$

Here $\tilde{\boldsymbol{\theta}}_n^{[0]}$ equals (12) with $\tilde{\boldsymbol{\mu}}_a = \mathbf{0}$ under H_0 , while $\tilde{\boldsymbol{\theta}}_n^{[1]}$ equals (12) with $\tilde{\boldsymbol{\mu}}_a = \tilde{\boldsymbol{\mu}}_a$ under

H_1 . $C_1 = 1/\sqrt{(2\pi)^m|\tilde{\Sigma}_b||\Sigma_e||\mathbf{H}|}$, $C_2 = 1/\sqrt{(2\pi)^m|K||\tilde{\Sigma}_b||\Sigma_e||\mathbf{A}||\mathbf{H} - \mathbf{C}\mathbf{A}^{-1}\mathbf{C}'|}$ are the constants. Some notations are defined as $\mathbf{A} = \mathbf{B}'_{aZ(n)}\Sigma_e^{-1}\mathbf{B}_{aZ(n)} + \mathbf{K}^{-1}$, $\mathbf{D} = \mathbf{X}'_{Z(n)}\Sigma_e^{-1}\mathbf{B}_{aZ(n)} + \boldsymbol{\mu}'_r\mathbf{K}^{-1}$, $\mathbf{C} = \mathbf{B}'_{bZ(n)}\Sigma_e^{-1}\mathbf{B}_{aZ(n)}$,
 $\mathbf{H} = \mathbf{B}'_{bZ(n)}\Sigma_e^{-1}\mathbf{B}_{bZ(n)} + \tilde{\Sigma}_b^{-1}$, $\mathbf{G}^{[0]} = \mathbf{X}'_{Z(n)}\Sigma_e^{-1}\mathbf{B}_{bZ(n)} + \tilde{\boldsymbol{\theta}}_n^{[0]'}\tilde{\Sigma}_b^{-1}$,
 $\mathbf{G}^{[1]} = \mathbf{X}'_{Z(n)}\Sigma_e^{-1}\mathbf{B}_{bZ(n)} + \tilde{\boldsymbol{\theta}}_n^{[1]'}\tilde{\Sigma}_b^{-1}$.

More derivation details are given in Appendix B.

By plugging (16) and (17) into PBF_n , we get the posterior Bayes factor, i.e.,

$$PBF_n = C_3 \sum_{\mathbf{r} \in \mathcal{R}} p(\mathbf{r}|H_1) \exp\left(-\frac{1}{2}(\boldsymbol{\mu}'_r\mathbf{K}^{-1}\boldsymbol{\mu}_r + \mathbf{G}^{[0]}\mathbf{H}^{-1}\mathbf{G}^{[0]'} - \mathbf{D}\mathbf{A}^{-1}\mathbf{D}' - (\mathbf{G}^{[1]} - \mathbf{D}\mathbf{A}^{-1}\mathbf{C}'))\right) \quad (18)$$

$$(\mathbf{H} - \mathbf{C}\mathbf{A}^{-1}\mathbf{C}')^{-1}(\mathbf{G}^{[1]} - \mathbf{D}\mathbf{A}^{-1}\mathbf{C}')' + \tilde{\boldsymbol{\theta}}_n^{[1]'}\tilde{\Sigma}_b^{-1}\tilde{\boldsymbol{\theta}}_n^{[1]} - \tilde{\boldsymbol{\theta}}_n^{[0]'}\tilde{\Sigma}_b^{-1}\tilde{\boldsymbol{\theta}}_n^{[0]}),$$

where $C_3 = \sqrt{|\mathbf{H}|/|K||\mathbf{A}||\mathbf{H} - \mathbf{C}\mathbf{A}^{-1}\mathbf{C}'|}$. By dropping out some constants or extra small terms in (18), it can be simplified. Furthermore, considering that under H_0 , the terms in each $\exp(\cdot)$ of (18) would be close to zero, we conduct Taylor expansion for further computation simplification.

Proposition 2. *After dropping out constants and extra small terms, we define the first order Taylor expansion of (18) as the final detection statistic Λ_n :*

$$\Lambda_n \equiv 2\tilde{\boldsymbol{\mu}}'_a\mathbf{B}'_{aZ(n)}(\mathbf{I} - \hat{\mathbf{H}})(\mathbf{X}_{Z(n)} - \mathbf{B}_{bZ(n)}\tilde{\boldsymbol{\theta}}_n^{[1]}) - \boldsymbol{\mu}'_a(\mathbf{B}'_{aZ(n)}\mathbf{B}_{aZ(n)} \circ \bar{\mathbf{A}})\boldsymbol{\mu}_a + \tilde{\boldsymbol{\mu}}'_a\mathbf{B}'_{aZ(n)}\hat{\mathbf{H}}\mathbf{B}_{aZ(n)}\tilde{\boldsymbol{\mu}}_a, \quad (19)$$

where $\hat{\mathbf{H}} = \mathbf{B}_{bZ(n)}(\mathbf{B}'_{bZ(n)}\mathbf{B}_{bZ(n)})^{-1}\mathbf{B}'_{bZ(n)}$ and $\bar{\mathbf{A}}$ has diagonal items $\bar{A}_{ii} = \alpha_i$, $i = 1, \dots, k_a$, and other items $\bar{A}_{ij} = \alpha_i\alpha_j$, $\forall i, j = 1, \dots, k_a$, $i \neq j$. More derivation details are given in Appendix B.

For (19), we can set a detection threshold h according to a pre-specific confidence level

(false alarm rate), and define that if $\Lambda_n > h$, the test statistic triggers an abnormal alarm. Otherwise, decide next $Z(n+1)$ and wait for \mathbf{X}_{n+1} .

4.4 Thompson Sampling for Sensor Selection

Now we talk about how to select $Z(n+1)$. In (19), denote $\mathbf{X}_{1Z(n)} = \mathbf{X}_{Z(n)} - \mathbf{B}_{bZ(n)}\tilde{\boldsymbol{\theta}}_n^{[1]}$. It indicates the estimated abnormal data for the selected dimensions $Z(n)$. When an anomaly occurs with abnormal dimension set Z^* , the more overlap between $Z(n+1)$ and Z^* , the more abnormal information $X_{1Z(n)}$ would take, and the larger value of Λ_{n+1} is expected to be. Consequently, at the present time point, we aim to select a subset $Z(n+1)$ which can maximize the expectation of Λ_{n+1} . This is similar to the CMAB problem (Chen et al. 2013), where $Z(n+1)$ is the super arm and Λ_{n+1} can be regarded as the reward function in our scenario. Following the Bayesian estimation framework, we propose to construct the sequential decision of $Z(n+1)$ based on Thompson sampling, which has been shown to perform competitively to the state of the arts in a variety of bandit and adaptive sampling problems (Agrawal and Goyal 2012, 2013). Under the framework of Thompson sampling, based on the current inference of \mathbf{X}_1 so far, the probability of \hat{Z} to maximize Λ_{n+1} is

$$\int \mathbb{I}\left(\hat{Z} = \arg \max_Z (\Lambda_{n+1} | Z, \mathbf{X}_1)\right) f(\mathbf{X}_1) d\mathbf{X}_1, \quad (20)$$

where \mathbb{I} is the indicator function and $f(\mathbf{X}_1)$ is the posterior distribution of \mathbf{X}_1 , which can be calculated from $\tilde{p}(\boldsymbol{\theta}_a, \mathbf{r})$. The core of the Thompson sampling is to sample a $\hat{\mathbf{X}}_1$ from $f(\mathbf{X}_1)$ instead of computing the integral in (20). This can be achieved by sampling a $\hat{\boldsymbol{\theta}}_a$ from $\tilde{p}(\boldsymbol{\theta}_a, \mathbf{r})$, sampling a $\hat{\mathbf{E}}$ from its distribution $N(\mathbf{0}, \boldsymbol{\Sigma}_e)$ and getting $\hat{\mathbf{X}}_1 = \mathbf{B}_a \hat{\boldsymbol{\theta}}_a + \hat{\mathbf{E}}$. Then select $Z(n+1)$ according to

$$Z(n+1) = \max_Z \Lambda_{n+1}(\hat{\mathbf{X}}_1) = 2\tilde{\boldsymbol{\mu}}_a' \mathbf{B}'_{aZ} (\mathbf{I} - \hat{\mathbf{H}}) \mathbf{B}_{aZ} \hat{\mathbf{X}}_1 - \boldsymbol{\mu}'_a (\mathbf{B}'_{aZ} \mathbf{B}_{aZ} \circ \bar{\mathbf{A}}) \boldsymbol{\mu}_a + \tilde{\boldsymbol{\mu}}_a' \mathbf{B}'_{aZ} \hat{\mathbf{H}} \mathbf{B}_{aZ} \tilde{\boldsymbol{\mu}}_a. \quad (21)$$

Hereafter we define the strategy of (21) as the oracle sampling procedure. The random sampling procedure encourages the exploration, and the maximization of Λ_{n+1} encourages the exploitation. Therefore, the proposed approach achieves good balance between exploration and exploitation. Furthermore, it has a good property that the regret between Z^* and $Z(n+1)$ converges to zero as n goes on. Though the strategy of (21) is desirable and can achieve good performance (as shown in Section 5.1), one limitation is that the sampling process requires large computation complexity, since $\Lambda_{n+1}(\hat{\mathbf{X}}_1)$ is a nonlinear function of $Z(n+1)$ and all the $\binom{p}{m}$ subsets need to be evaluated for best selection. This is a common problem for many CMAB strategies (Chen et al. 2016), where they usually assume an oracle computer center can evaluate all the combinations. However, enumerating all possible combinations of the arms is intractable especially when the number of arms is large. Therefore, we would like to reduce the complexity of the CMAB problem through the following proposition.

Proposition 3. *Suppose any column of \mathbf{B}_a or \mathbf{B}_b , denoted as \mathbf{b} , satisfies $\|\mathbf{b}^2\|_\infty \leq \frac{c}{p}\|\mathbf{b}\|_2^2$, where $c \in \mathbb{R}_+$ is a constant satisfying $1 \leq c \leq p$. Let $\epsilon, \delta \in (0, 1]$ be two small values, and let $\frac{c^2}{2\epsilon^2} \log\left(\frac{(k_a+k_b)^2}{\delta}\right) \leq m \leq \frac{2a_p^2 p^2 \epsilon^2}{c^2 \log\left(\frac{(k_a+k_b)^2}{\delta}\right)}$ be an integer, where a_p is the smallest probability that a variable can be sampled. For all possible m -dimensional subsets Z in $\mathcal{Z} = \{Z_k, k = 1, \dots, M\}$ where $M = \binom{p}{m}$, with probability at least $1 - 2\delta$, for any column \mathbf{b}_{ai} of \mathbf{B}_a and any column \mathbf{b}_{bj} of \mathbf{B}_b , we have*

$$-a_p \epsilon \leq \mathbf{b}'_{aiZ} \mathbf{b}_{bjZ} \leq a_1 \epsilon,$$

where $0 \leq a_p \leq a_1 \leq 1$ are small constants. This indicates $\mathbf{B}'_{bZ} \mathbf{B}_{aZ} = \mathbf{0}$ are approximately valid. The verification details are shown in Appendix C.

Under Proposition 3, the sampling procedure of (21) can be further simplified as:

$$\begin{aligned} Z(n+1) &= \max_Z \Lambda_{n+1}(\hat{\mathbf{X}}_1) = 2\tilde{\boldsymbol{\mu}}_a' \mathbf{B}'_{aZ} \mathbf{B}_{aZ} \hat{\mathbf{X}}_1 - \boldsymbol{\mu}'_a (\mathbf{B}'_{aZ} \mathbf{B}_{aZ} \circ \bar{\mathbf{A}}) \boldsymbol{\mu}_a \\ &= \sum_{i \in Z} \left(2\hat{\mathbf{X}}_1' \mathbf{B}'_{ai} \mathbf{B}_{ai} \tilde{\boldsymbol{\mu}}_a - \boldsymbol{\mu}'_a (\mathbf{B}'_{ai} \mathbf{B}_{ai} \circ \bar{\mathbf{A}}) \boldsymbol{\mu}_a \right), \end{aligned} \quad (22)$$

where \mathbf{B}_{ai} is the i^{th} row of \mathbf{B}_a . This indicates that we only need to rank

$$\Lambda_{(n+1)i} = 2\hat{\mathbf{X}}_1' \mathbf{B}'_{ai} \mathbf{B}_{ai} \tilde{\boldsymbol{\mu}}_a - \boldsymbol{\mu}'_a (\mathbf{B}'_{ai} \mathbf{B}_{ai} \circ \bar{\mathbf{A}}) \boldsymbol{\mu}_a, i = 1, \dots, p \quad (23)$$

from the largest to the smallest and select the top m items, instead of enumerating all the possible sets of Z . Hereafter we denote (22) as the simplified sampling procedure. Consequently, the complexity of sampling process drops dramatically and allows us to handle very high dimensional data. The simplified procedure of Thompson sampling is shown in Algorithm 2 with the total computation for one time point as $O(p \log(p))$.

Algorithm 2: Simplified Thompson Sampling Procedure

Input: $\tilde{p}(\boldsymbol{\theta}_a, \mathbf{r})$, $\tilde{\boldsymbol{\mu}}_a$, $\boldsymbol{\mu}_a$, $\mathbf{B}_{aZ(n)}$, $\bar{\mathbf{A}}$, $\boldsymbol{\Sigma}_e$ estimated upon to the current time point n

Output: $Z(n+1)$

Sample $\hat{\boldsymbol{\theta}}_a \sim \tilde{p}(\boldsymbol{\theta}_a, \mathbf{r})$, sample $\hat{\mathbf{E}}$ from $N(\mathbf{0}, \boldsymbol{\Sigma}_e)$ and get $\hat{\mathbf{X}}_1 = \mathbf{B}_a \hat{\boldsymbol{\theta}}_a + \hat{\mathbf{E}}$

Compute $\Lambda_{(n+1)i} = 2\hat{\mathbf{X}}_1' \mathbf{B}'_{ai} \mathbf{B}_{ai} \tilde{\boldsymbol{\mu}}_a - \boldsymbol{\mu}'_a (\mathbf{B}'_{ai} \mathbf{B}_{ai} \circ \bar{\mathbf{A}}) \boldsymbol{\mu}_a$, $i = 1, 2, \dots, p$

Rank the $\Lambda_{(n+1)i}$, for $i = 1, 2, \dots, p$ from the largest to the smallest, and select the top m items as $Z(n+1)$

4.5 Theoretical Properties

Now we discuss some theoretical properties of the simplified Thompson sampling procedure under asymptotic conditions. These properties are built upon the asymptotic properties of variation Bayesian inferences in Wang and Blei (2019). We first consider the specific cases when there is no background information $\mathbf{B}_t \boldsymbol{\theta}_n$ in the data stream. In this case, we do not need to estimate $\boldsymbol{\theta}_n$ at all, and can directly set (12) and (13) to be zero.

Theorem 1. For a system without background information, i.e., $\mathbf{B}_b\boldsymbol{\theta}_n = \mathbf{0}$, when there is no change in the system, as $n \rightarrow \infty$, we have $q_j(\theta_{aj}) \xrightarrow{d} \delta_0, \forall j = 1 \dots k_a$, where δ_0 is a point mass at 0. This means $\mu_{aj} \rightarrow 0$ and $s_j^2 \rightarrow 0$. Consequently we have $E(\Lambda_{(n+1)i}) \rightarrow 0$ and $Var(\Lambda_{(n+1)i}) \rightarrow 0, \forall i = 1 \dots p$.

More details are shown in Appendix D. Theorem 1 indicates that when the system has no change, under the limit conditions, Algorithm 2 can select $Z(n+1)$ from all variables randomly.

Theorem 2. For a system without background information, i.e., $\mathbf{B}_b\boldsymbol{\theta}_n = \mathbf{0}$, when the system has change, assume the change relates to certain bases $\mathcal{A} \subset \{1, \dots, k_a\}$ with change magnitude $\phi_l, l \in \mathcal{A}$. As $n \rightarrow \infty$, $q_l(\theta_{al}) \xrightarrow{d} \delta_{\phi_l}$ for $l \in \mathcal{A}$ where δ_{ϕ_l} is a point mass at ϕ_l , and $q_j(\theta_{aj}) \xrightarrow{d} \delta_0, \forall j \notin \mathcal{A}$. This means $\mu_{al} \rightarrow \phi_l, \alpha_l \rightarrow 1$ and $s_l^2 \rightarrow 0, \forall l \in \mathcal{A}$. As to other bases, $\mu_{aj} \rightarrow 0$ and $s_j^2 \rightarrow 0, \forall j \notin \mathcal{A}$. Consequently, $E(\Lambda_{(n+1)i}) \rightarrow \sum_{l \in \mathcal{A}} B_{ail}^2 \phi_l^2 + 2 \sum_{l_1, l_2 \in \mathcal{A}, l_1 \neq l_2} B_{ail_1} B_{ail_2} \phi_{l_1} \phi_{l_2}$ and $Var(\Lambda_{(n+1)i}) \rightarrow 0, \forall i = 1 \dots p$.

More details are shown in Appendix D. Theorem 2 indicates that in abnormal condition, we prefer to choose the variables mostly influenced by the abnormal patterns.

As to general cases with background information, we have the following Corollary 3, where the condition $m \rightarrow \infty$ is to guarantee $\boldsymbol{\theta}_n$ can be estimated accurately. Then the properties of estimated $\boldsymbol{\theta}_a$ together with $\Lambda_{(n+1)i}$ in Theorem 1 and Theorem 2 can be guaranteed.

Corollary 3. For a general system with background information $\mathbf{B}_b\boldsymbol{\theta}_n$, under $p \rightarrow \infty, m \rightarrow \infty$ (but m/p can be bounded or go to infinity), the results of Theorem 1 and Theorem 2 hold.

Hereafter, we shorten our proposed Composite Decomposition based Spike and Slab Detection scheme using oracle sampling procedure as CDSSD(O) and using simplified sampling procedure as CDSSD. The full detection scheme is shown in Algorithm 3.

Remark 1. *It is to be noted that in some real applications where the prior information of \mathbf{B}_a is unknown and not inferable, \mathbf{B}_a can be simply set to be identity matrix $\mathbf{B}_a = \mathbf{I} \in \mathcal{R}^{p \times p}$. In this case it aims to detect sparse changes on the original p dimensions directly.*

Algorithm 3: Composite Decomposition based Change Detection

Input: Data streams $\mathbf{X}_n, n = 1, \dots$

Set the initial sampling set $Z(1)$ by randomly selecting m variables out of the p variables.

for $n = 1, \dots$ **do**

 Collect the data $\mathbf{X}_{Z(n)}$ Update posterior distributions via Algorithm 1.

 Calculate the detection statistic Λ_n via Eq (19).

if $\Lambda_n > h$ **then**

 | Trigger a change alarm

else

 | Decide the next sampling set $Z(n + 1)$ via Algorithm 2.

5 Numerical Studies

In this section, we conduct extensive experiments on both synthetic and real-world data sets to evaluate the performance of our proposed CDSSD. We also compare it with the following existing baselines:

TRAS: top-r adaptive sampling detection algorithm in Liu et al. (2015).

NAS: nonparametric anti-rank adaptive sampling algorithm in Xian et al. (2017).

CMAB(s): simplified combinatorial multi-armed bandit adaptive sampling strategy in Zhang and Hoi (2019).

SASAM: spatial-adaptive sampling and monitoring procedure in Wang et al. (2018a).

CDSSD(I): a variant strategy of CDSSD, which sets the anomaly bases \mathbf{B}_a to be the identity matrix. This represents cases when \mathbf{B}_a is neither known nor inferable.

ORACLE: the proposed detection scheme yet assuming all the p variables are fully observable at each time point and no adaptive sampling is required. It is used as a performance upper bound of our detection scheme.

5.1 Efficiency comparison between CDSSD and CDSSD(O)

We first evaluate the performance difference between CDSSD and CDSSD(O) and show that the simplification of CDSSD has little influence to the detection power, and yet can save a lot of computation. At the same time, we also compare them with the combinatorial multi-armed bandit (CMAB) method proposed by [Zhang and Hoi \(2019\)](#). Because of high computation complexity of CDSSD(O) and CMAB(s), we only use low dimensions of $p = 15, m = 5, 8, 11$, and compare ADDs of these three strategies.

In our simulation, we assume $\mathbf{B}_b \in R^{15 \times 3}$ are the three lowest frequency Fourier bases and $\mathbf{B}_a \in R^{15 \times 10}$ are 10 four-order B-spline bases with 14 equally spaced knots. When the data is normal, $\boldsymbol{\theta}_t \sim N(\mathbf{0}, \boldsymbol{\Sigma}_b)$ with $\boldsymbol{\Sigma}_b = \sigma_b^2 \mathbf{I}$ and $\sigma_b = 0.3$. $\mathbf{E}_t \sim N(\mathbf{0}, \boldsymbol{\Sigma}_e)$ with $\boldsymbol{\Sigma}_e = \sigma_e^2 \mathbf{I}$ and $\sigma_e = 0.05$. When a change occurs after the change point $\tau = 50$, we assume only the j^{th} column of the 10 B-spline bases has nonzero coefficient $\theta_{aj} = \phi$, where ϕ is the change magnitude. For each simulation replication, we set j by randomly drawing a number from 1 to 10, and generate random samples of $\mathbf{X}_t = \mathbf{B}_b \boldsymbol{\theta}_t + \mathbf{B}_a \boldsymbol{\theta}_a + \mathbf{E}_t$ for a total time length $T = 2000$ from the above experimental settings. For CMAB(s), the parameters are set according to the algorithm in [Zhang and Hoi \(2019\)](#). For CDSSD, we set $\lambda = 0.1$, $w_j = 0.1$, $\sigma_j = 3$ for $j = 1, \dots, k_a$, and $v = 10^{-7}$. For all the methods, we tune their detection thresholds to ensure that their ARL_0 is exactly 200 such that their detection performance under change cases can be fairly compared. Then we record the first time point that each algorithm triggers a change alarm as its corresponding detection delay. We calculate ADD using 1000 replications, as the performance evaluation criterion of different methods.

The results are shown in [Table 1](#). We can see that both CDSSD(O) and CDSSD strongly outperform CMAB(s) in all ϕ 's magnitudes and m/p settings, demonstrating the superiority of our proposed methods. The difference between CDSSD(O) and CDSSD is not significant. Only when m/p is quite small and the magnitude of defect ϕ is quite small, the gap between CDSSD and CDSSD(O) is obvious. In other cases, CDSSD performs almost as well as

CDSSD(O). This indicates that in most scenarios, CDSSD can be served as a substitute of CDSSD(O). Therefore in the following experiments, we only compare CDSSD with other state-of-the-art methods for performance evaluation for computation reduction.

Table 1: ADDs (and Standard Deviation of Detection Delays, i.e., STDs in the abbreviation) for Experiments of $\mathbf{X}_t \in \mathcal{R}^{15 \times 1}$.

ϕ	$p = 15, m = 5$			$p = 15, m = 8$			$p = 15, m = 11$		
	CDSSD	CDSSD(O)	CMAB(s)	CDSSD	CDSSD(O)	CMAB(s)	CDSSD	CDSSD(O)	CMAB(s)
0.0	200(251)	200(227)	200(187)	200(267)	200(273)	200(187)	200(295)	200(272)	200(193)
0.1	30.3(37.4)	16.4 (16.8)	59.6(51.6)	13.2(15.2)	9.00 (9.29)	21.8(13.6)	7.06(7.73)	5.94 (5.89)	12.9(7.22)
0.2	8.16(7.59)	5.76 (4.58)	24.3(16.6)	3.91(3.39)	3.17 (2.24)	8.41(4.10)	2.48(2.08)	2.07 (1.36)	5.02(1.84)
0.3	4.58(4.05)	3.73 (2.68)	14.7(9.23)	2.20(1.62)	1.96 (1.16)	5.42(2.51)	1.56(1.03)	1.39 (0.68)	3.29(1.19)
0.4	3.49(2.73)	2.79 (2.11)	10.5(6.62)	1.77(1.29)	1.59 (0.93)	3.88(1.69)	1.28(0.70)	1.19 (0.48)	2.47(0.76)
0.5	2.87(2.35)	2.53 (2.07)	8.22(5.36)	1.60(1.25)	1.41 (0.76)	3.01(1.37)	1.25(0.68)	1.12 (0.41)	1.96(0.62)
0.6	2.50(1.93)	2.17 (1.67)	6.37(4.24)	1.47(1.04)	1.33 (0.67)	2.54(1.24)	1.21(0.69)	1.10 (0.41)	1.96(0.62)
0.7	2.23(1.67)	2.06 (1.46)	5.38(3.68)	1.39(0.94)	1.31 (0.72)	2.15(1.12)	1.19(0.67)	1.07 (0.28)	1.44(0.55)
0.8	2.11(1.57)	1.93 (1.50)	4.71(3.15)	1.39(0.96)	1.23 (0.60)	1.92(0.93)	1.15(0.58)	1.07 (0.33)	1.23(0.43)
0.9	2.09(1.72)	1.80 (1.27)	4.26(2.89)	1.32(0.82)	1.22 (0.60)	1.79(0.93)	1.15(0.63)	1.07 (0.31)	1.14(0.38)
1.0	1.96(1.50)	1.79 (1.26)	3.57(2.38)	1.30(0.86)	1.16 (0.50)	1.61(0.76)	1.11(0.46)	1.06 (0.29)	1.07(0.27)

5.2 One-Dimensional(1D) Experiments

In this section, we consider higher dimensional cases with $\mathbf{X}_t \in \mathcal{R}^{30 \times 1}$. We assume $\mathbf{B}_b \in R^{30 \times 2}$ are the two lowest frequency Fourier bases and $\mathbf{B}_a \in R^{30 \times 17}$ are 17 four-order B-spline bases with 21 equally spaced knots. All the other experimental parameters including $\theta_b, \theta_a, \mathbf{E}_t$ are generated in the same way as Section 5.1. As to other baseline methods, for TRAS, we set its parameters $r = m, \mu_{min} = 0.05$ and $\Delta = 0.0001$ according to recommendation of Liu et al. (2015). For NAS, we set $k = 0.05, \Delta = 0.07$ following the algorithm in Xian et al. (2017). For SASAM, the parameters are selected to be $\theta_1 = 0.1, \theta_2 = 0.7, h = 1$ and $\mu_{min} = 0.1$ according to the recommendations of Wang et al. (2018a).

The detection results for ϕ ranging from 0 to 1 with $m = 10, 20$ and 30 are shown in Figures 1a, 1b and 1c respectively. The detailed values together with their standard deviations are shown in Appendix E. Clearly, except ORACLE, which is infeasible in practice, CDSSD has the smallest ADD generally, followed by CDSSD(I), demonstrating their detection power

of our proposed detection framework. In particular, for small ϕ , CDSSD performs better than CDSSD(I), while for large ϕ , is slightly inferior to CDSSD(I). This is because for small ϕ , the change pattern as a whole contributes to the detection. While when ϕ is larger, it is certain individual dimensions distinctly influenced by anomaly patterns that contribute to the detection statistic mostly. Consequently CDSSD(I) with identity \mathbf{B}_a can also have satisfactory detection performance. CMAB(s) performs a little inferiorly compared with CDSSD or CDSSD(I), followed by SASAM. As to CUSUM and NAS, their performances are not very satisfactory, since they do not consider either correlations of different variables or change sparsity.

5.3 Extension to Two-Dimensional (2D) Experiments

In this experiment, we further consider data with more complex spatial structure, i.e., \mathbf{X}_t as an image with 20×20 pixels. We first generate each column of $\mathbf{b}_b \in \mathcal{R}^{20 \times 2}$ from two-order B-spline bases with 4 equally spaced knots, and set $\mathbf{B}_b = \mathbf{b}_b \otimes \mathbf{b}_b$, where \otimes is the Kronecker tensor product. Similarly, we generate each column of $\mathbf{b}_a \in \mathcal{R}^{20 \times 9}$ from four-order B-spline bases with 13 equally spaced knots, and set $\mathbf{B}_a = \mathbf{b}_a \otimes \mathbf{b}_a$. All the other experimental parameters including $\boldsymbol{\theta}_b$, $\boldsymbol{\theta}_a$, \mathbf{E}_t are generated in the same way as Section 5.1.

We also tune the change magnitude ϕ and evaluate the performance of different algorithms according to their ADDs. We vectorize each \mathbf{X}_t as a vector with $p = 400$ to construct the detection statistics for all the methods. The performance of different methods under $m = 20$, 40 and 60 is shown in Figures 2a, 2b and 2c. The specific ADD values together with their standard deviations are added in Appendix E. Similar as the result in Section 5.2, CDSSD performs the best generally, but is slightly inferior to CDSSD(I) when m/p is small and ϕ is large, due to the same reason as Section 5.2. However, its gap from ORACLE is larger than that of one dimensional case in Section 5.2. This is because the proportion of observable dimensions, i.e., m/p , is much smaller than that of one dimensional case. In addition, other

methods, i.e., CMAB(s), SASAM, CUSUM and NAS perform worse than CDSSD and even CDSSD(I).

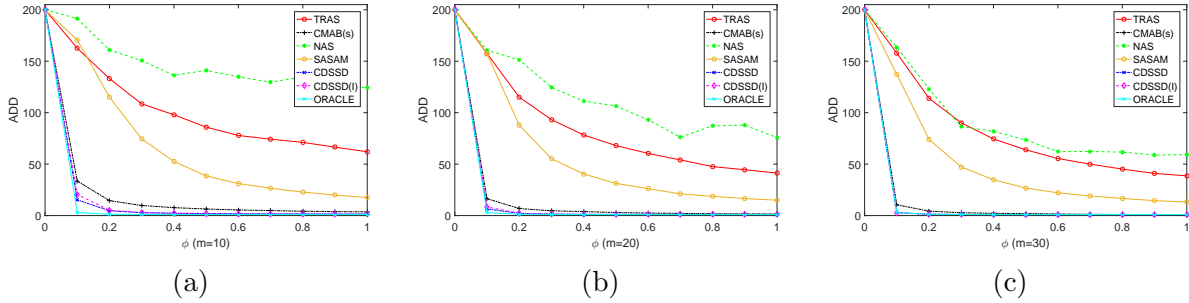


Figure 1: ADDs for 1D experiments with (a) $m = 10$, (b) $m = 20$, (c) $m = 30$

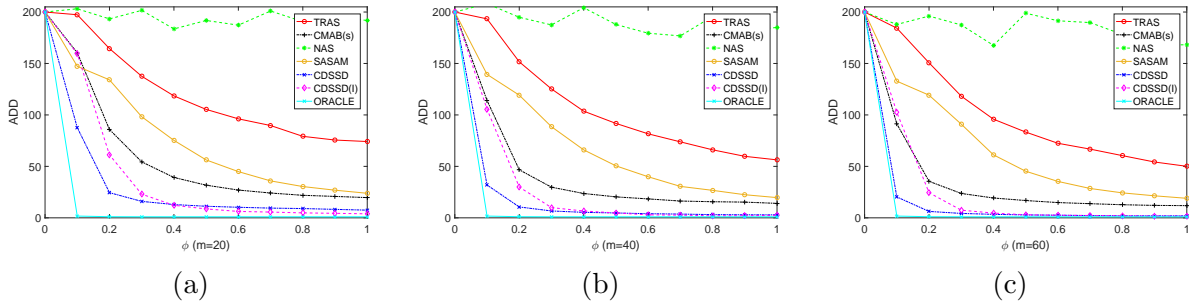


Figure 2: ADDs for 2D experiments with (a) $m = 20$, (b) $m = 40$, (c) $m = 60$

5.4 Case Study on Solar Flare Detection

We apply CDSSD to a real case study, i.e., the solar flare detection with the same data set as Liu et al. (2015); Wang et al. (2018a). The data set is in video format and contains 300 frames of sequential images, each of which have 67744 pixels distributed on a 232×292 grid. By treating one pixel as a dimension, the total vectorized data have dimension 67744. The solar flare appears at time $t = 187 \sim 202$ in this data set. We use the first 100 frames as training data for parameter estimation. In particular, we conduct principal component analysis for $t = 1, \dots, 10$, and extract the first 20 principal components as the dictionary of normal bases, i.e., $\mathbf{B}_b \in \mathcal{R}^{67,744 \times 20}$, The extracted PCA scores represent $\boldsymbol{\theta}_t$, and can be used to further compute the prior covariance matrix of $\boldsymbol{\theta}_t$, i.e., $\boldsymbol{\Sigma}_b$, and the standard deviation of

noise, i.e., $\sigma_e = 0.0319$. As for the anomaly bases, it is desirable to construct \mathbf{B}_a according to the size and shape of possible patterns, which can be obtained from historical abnormal data when solar flares occur. Consider that the pattern of solar flare approximates to small circle piles, and forms many free shapes by these circle piles. According to this prior information, we generate $\mathbf{B}_a \in \mathcal{R}^{67,744 \times 256}$ from three-order B-spline bases with 19 equally spaced knots.

We assume that only 400 out of 67744 pixels are available in our case, while Liu et al. (2015) assumed 2000 out of 67744 observable and Wang et al. (2018a) set 500 out of 67744 pixels observable. To show the detection efficacy of CDSSD, we compare it with the other methods in this literature. We set $ARL_0 = 1100$ according to Wang et al. (2018a) for all the methods. According to the requirements in (Liu et al. 2015), the parameters of TRAS are selected to be $\mu_{min} = 2.1$ and $\Delta = 5 * 10^{-6}$. The parameters of SASAM are set to be $\theta_1 = 0.1$, $\theta_2 = 0.4$, $h = 5$ and $\mu_{min} = 2$ according to recommendations in (Wang et al. 2018a). As for NAS, the parameters are selected $\Delta = 1.47 * 10^{-5}$, $k = 0.1$, $\lambda = 1.6 * 10^{-3}$ and $\lambda_0 = 0.0103$ according to (Xian et al. 2017). For our method CDSSD, we set the parameters $\sigma_j = 10$, $w_j = 0.1$ for $j = 1, 2, \dots, k_a$ and $\lambda = 0.1$ according to the requirements of the algorithm. Here we don't compare with CMAB(s) in (Zhang and Hoi 2019) since in CMAB(s), we need to construct the covariance matrix of size of 67744×67744 . That requires more than 32 GB memory of computer, which is really time-consuming to implement and thus inefficient for online detection.

The monitoring process starts from $t = 101$. The DDs(Detection Delay) of the four methods are $DD_{CDSSD} = 2$, $DD_{TRAS} = 10$, $DD_{SASAM} = 19$ and $DD_{NAS} = 22$ respectively. Their detection statistics are shown in Figure 3. As we can see, CDSSD has the smallest DD= 2, outperforming other methods and achieving efficient online anomaly detection. To better illustrate the performance of CDSSD, we visualize its detection results of three selected time points $t = 180, 188$ and 192 . When the anomaly has not occur at $t = 180$, Figure 4 (a) shows the figure of sun's surface in normal condition. The detection result indicates that there is no fitted anomaly pattern in Figure 4 (c) and the sampling points are distributed

randomly in Figure 4 (d). After the solar flare occurs at $t = 186$ which is strengthened in red circle in Figure 5 (a) and Figure 6 (a), At $t = 188$, CDSSD first detects the anomaly. As we can see, there appears a fitted anomaly pattern in Figure 5 (c) and the sampling points concentrate at the area of the solar flare in Figure 5 (d). To show this is not a short-time concentration like random sampling, we further check the detection results after triggering an alarm, e.g., at $t = 192$. The detection results are the same as that of $t = 188$. So we can conclude that before anomaly appears, CDSSD searches all the variables randomly and does not concentrate any set of variables. However, after anomaly appears, CDSSD can concentrate on the variables influenced by the anomaly for a period of time.

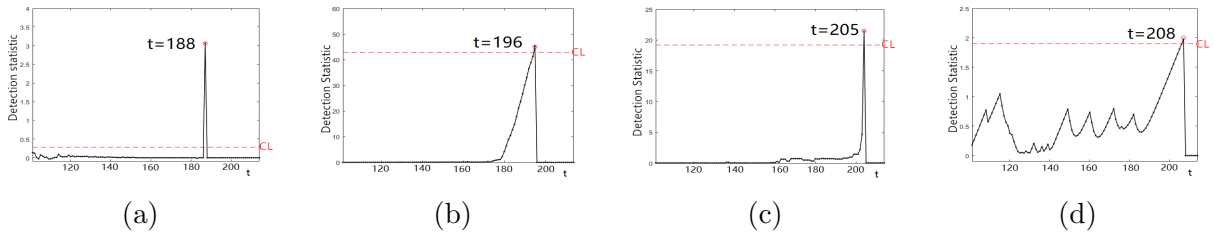


Figure 3: Detection statistics for solar flare case (a) $DD_{CDSSD} = 2$, (b) $DD_{TRAS} = 10$, (c) $DD_{SASAM} = 19$ and (d) $DD_{NAS} = 22$.

6 Conclusions

This paper addresses high dimensional sequential change detection problem with partial observations. It proposes an adaptive sampling method to select a subset of variables in the system for online monitoring. Specifically, to deal with the correlations among variables and sparse changes in the system, we introduce the framework of sparse smooth composite decomposition, based on which we learn the value of parameters via spike and slab variational Bayesian inference. To be coherent, using the estimated parameters, we construct the posterior Bayesian factor as our detection statistic. By formulating the detection statistic as the reward function in multi-armed bandit problem, we propose a Thompson sampling strategy for sampling the most informative variables for the next time point. This sampling strategy can achieve two desirable properties, (1) randomly sampling among variables when

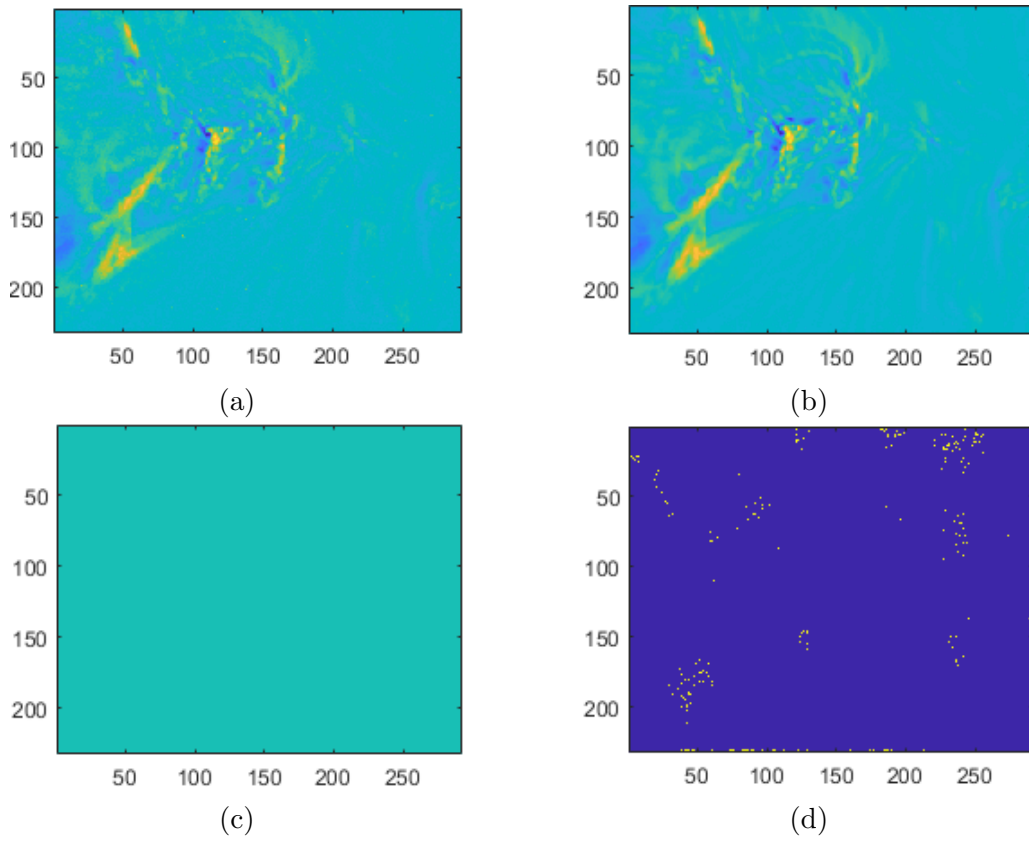


Figure 4: Detection results of solar flare case at $t = 180$.(a) Original data (b) Fitted normal data (c) Fitted abnormal data (d) Sampling points

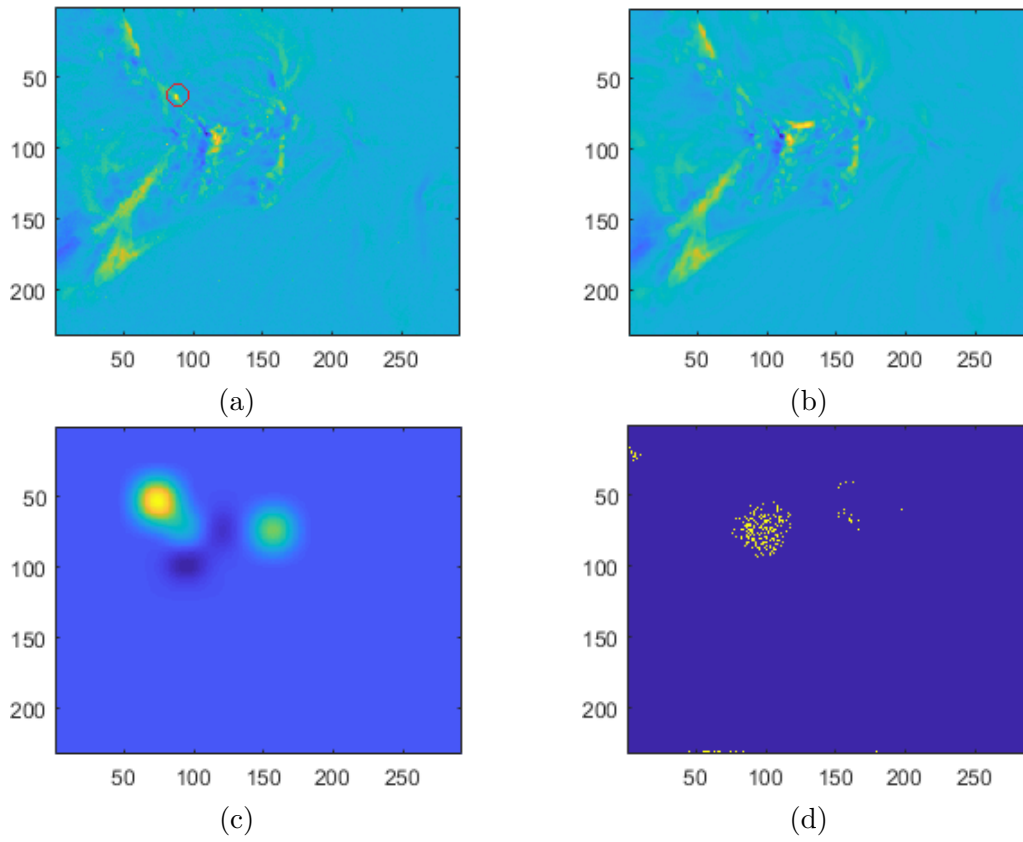


Figure 5: Detection results of solar flare case at $t = 188$.(a) Original data (b) Fitted normal data (c) Fitted abnormal data (d) Sampling points

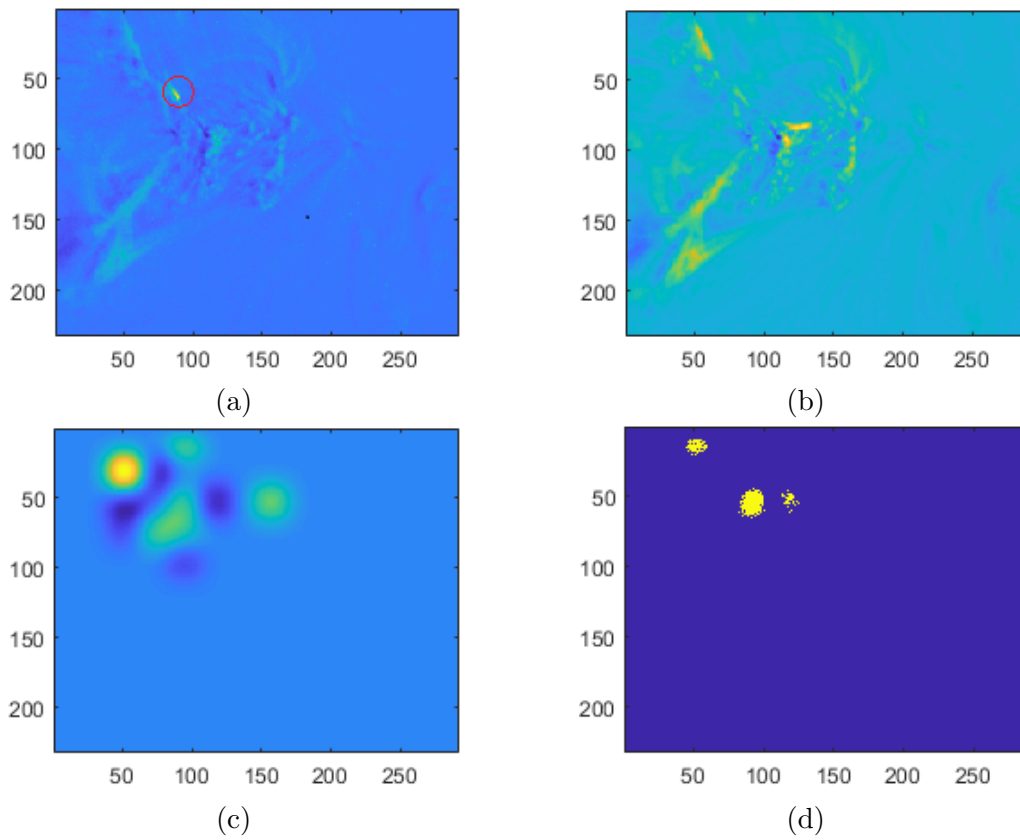


Figure 6: Detection results of solar flare case at $t = 192$. (a) Original data (b) Fitted normal data (c) Fitted abnormal data (d) Sampling points

the process is normal and (2) sampling anomalous points preferentially and consistently when change appears in the system. So it can achieve good exploration and exploitation property, which contributes greatly to the efficiency of our proposed algorithm. Finally, through synthetic and real-world data experiments, we conclude that our method performs much better than existing adaptive sampling strategies. In the area of online process monitoring, this research develops an novel adaptive sampling strategy to determine which subset of data streams should be observed when only a limited number of resources are available. The applications of our proposed method are extensive, such as syndromic surveillance in epidemiology, network traffic control and surveillance video.

References

- Agrawal, S. and Goyal, N. (2012), “Analysis of thompson sampling for the multi-armed bandit problem,” in *Conference on learning theory*, pp. 39–1.
- (2013), “Thompson sampling for contextual bandits with linear payoffs,” in *International Conference on Machine Learning*, pp. 127–135.
- Aitkin, M. (1991), “Posterior bayes factors,” *Journal of the Royal Statistical Society: Series B (Methodological)*, 53, 111–128.
- Attias, H. (2000), “A variational bayesian framework for graphical models,” in *Advances in neural information processing systems*, pp. 209–215.
- Ba, S., Joseph, V. R., et al. (2012), “Composite Gaussian process models for emulating expensive functions,” *The Annals of Applied Statistics*, 6, 1838–1860.
- Bubeck, S., Wang, T., and Viswanathan, N. (2013), “Multiple identifications in multi-armed bandits,” in *International Conference on Machine Learning*, pp. 258–265.
- Cai, T. T., Ren, Z., Zhou, H. H., et al. (2016), “Estimating structured high-dimensional covariance and precision matrices: Optimal rates and adaptive estimation,” *Electronic Journal of Statistics*, 10, 1–59.

- Cao, Y., Wen, Z., Kveton, B., and Xie, Y. (2019), “Nearly optimal adaptive procedure with change detection for piecewise-stationary bandit,” in *The 22nd International Conference on Artificial Intelligence and Statistics*, pp. 418–427.
- Carbonetto, P., Stephens, M., et al. (2012), “Scalable variational inference for Bayesian variable selection in regression, and its accuracy in genetic association studies,” *Bayesian analysis*, 7, 73–108.
- Chan, H. P. (2017), “Optimal sequential detection in multi-stream data,” *The Annals of Statistics*, 45, 2736–2763.
- Chen, W., Wang, Y., and Yuan, Y. (2013), “Combinatorial multi-armed bandit: General framework and applications,” in *International Conference on Machine Learning*, pp. 151–159.
- Chen, W., Wang, Y., Yuan, Y., and Wang, Q. (2016), “Combinatorial multi-armed bandit and its extension to probabilistically triggered arms,” *The Journal of Machine Learning Research*, 17, 1746–1778.
- Cheng, M., Jing, L., and Ng, M. K. (2018), “Tensor-based low-dimensional representation learning for multi-view clustering,” *IEEE Transactions on Image Processing*, 28, 2399–2414.
- Dasgupta, S. and Gupta, A. (1999), “An elementary proof of the Johnson-Lindenstrauss lemma,” *International Computer Science Institute, Technical Report*, 22, 1–5.
- Durand, A. and Gagné, C. (2014), “Thompson sampling for combinatorial bandits and its application to online feature selection,” in *Workshops at the Twenty-Eighth AAAI Conference on Artificial Intelligence*.
- Even-Dar, E., Mannor, S., and Mansour, Y. (2006), “Action elimination and stopping conditions for the multi-armed bandit and reinforcement learning problems,” *Journal of machine learning research*, 7, 1079–1105.
- Fan, J., Fan, Y., and Lv, J. (2008), “High dimensional covariance matrix estimation using a factor model,” *Journal of Econometrics*, 147, 186–197.

- Ghosh, J. K., Delampady, M., and Samanta, T. (2007), *An introduction to Bayesian analysis: theory and methods*, Springer Science & Business Media.
- Hoeffding, W. (1994), “Probability inequalities for sums of bounded random variables,” in *The Collected Works of Wassily Hoeffding*, Springer, pp. 409–426.
- Kass, R. E. and Raftery, A. E. (1995), “Bayes factors,” *Journal of the american statistical association*, 90, 773–795.
- Liu, F., Lee, J., and Shroff, N. (2018), “A change-detection based framework for piecewise-stationary multi-armed bandit problem,” in *Thirty-Second AAAI Conference on Artificial Intelligence*.
- Liu, K., Mei, Y., and Shi, J. (2015), “An adaptive sampling strategy for online high-dimensional process monitoring,” *Technometrics*, 57, 305–319.
- Mei, Y. (2010), “Efficient scalable schemes for monitoring a large number of data streams,” *Biometrika*, 97, 419–433.
- Meier, L., Van de Geer, S., Bühlmann, P., et al. (2009), “High-dimensional additive modeling,” *The Annals of Statistics*, 37, 3779–3821.
- Mitchell, T. J. and Beauchamp, J. J. (1988), “Bayesian variable selection in linear regression,” *Journal of the American Statistical Association*, 83, 1023–1032.
- Mo, X., Monga, V., Bala, R., and Fan, Z. (2013), “Adaptive sparse representations for video anomaly detection,” *IEEE Transactions on Circuits and Systems for Video Technology*, 24, 631–645.
- Montgomery, D. C. (2007), *Introduction to statistical quality control*, John Wiley & Sons.
- Morey, R. D. and Rouder, J. N. (2011), “Bayes factor approaches for testing interval null hypotheses.” *Psychological methods*, 16, 406.
- Qi, N., Shi, Y., Sun, X., Wang, J., Yin, B., and Gao, J. (2017), “Multi-dimensional sparse models,” *IEEE transactions on pattern analysis and machine intelligence*, 40, 163–178.

- Wang, A., Xian, X., Tsung, F., and Liu, K. (2018a), “A spatial-adaptive sampling procedure for online monitoring of big data streams,” *Journal of Quality Technology*, 50, 329–343.
- Wang, H., Sievert, S., Liu, S., Charles, Z., Papailiopoulos, D., and Wright, S. (2018b), “Atomo: Communication-efficient learning via atomic sparsification,” in *Advances in Neural Information Processing Systems*, pp. 9850–9861.
- Wang, K. and Jiang, W. (2009), “High-dimensional process monitoring and fault isolation via variable selection,” *Journal of Quality Technology*, 41, 247–258.
- Wang, Y. and Blei, D. M. (2019), “Frequentist consistency of variational Bayes,” *Journal of the American Statistical Association*, 114, 1147–1161.
- Wang, Y. and Mei, Y. (2013), “Monitoring multiple data streams via shrinkage post-change estimation,” *Annals of Statistics*.
- Wasserman, L. (2000), “Bayesian model selection and model averaging,” *Journal of mathematical psychology*, 44, 92–107.
- Wood, S. N., Goude, Y., and Shaw, S. (2015), “Generalized additive models for large data sets,” *Journal of the Royal Statistical Society: Series C (Applied Statistics)*, 64, 139–155.
- Xian, X., Wang, A., and Liu, K. (2017), “A Nonparametric Adaptive Sampling Strategy for Online Monitoring of Big Data Streams,” *Technometrics*, 1–12.
- Xian, X., Zhang, C., Bonk, S., and Liu, K. (2019), “Online monitoring of big data streams: A rank-based sampling algorithm by data augmentation,” *Journal of Quality Technology*, 1–19.
- Xu, R., Xu, Y., and Quan, Y. (2020), “Factorized Tensor Dictionary Learning for Visual Tensor Data Completion,” *IEEE Transactions on Multimedia*.
- Yan, H., Paynabar, K., and Shi, J. (2017), “Anomaly detection in images with smooth background via smooth-sparse decomposition,” *Technometrics*, 59, 102–114.

- Zhang, C. and Hoi, S. C. (2019), “Partially Observable Multi-Sensor Sequential Change Detection: A Combinatorial Multi-Armed Bandit Approach,” in *Proceedings of the AAAI Conference on Artificial Intelligence*, vol. 33, pp. 5733–5740.
- Zhang, C., Yan, H., Lee, S., and Shi, J. (2018), “Weakly correlated profile monitoring based on sparse multi-channel functional principal component analysis,” *IIE Transactions*, 50, 878–891.
- Zhang, K. and Zhang, L. (2018), “Supervised Dictionary Learning with Smooth Shrinkage for Image Denoising,” *Neural Processing Letters*, 47, 535–548.
- Zhang, L., Wang, K., and Chen, N. (2016), “Monitoring wafers’ geometric quality using an additive Gaussian process model,” *IIE Transactions*, 48, 1–15.
- Zhuang, H., Wang, C., and Wang, Y. (2017), “Identifying outlier arms in multi-armed bandit,” in *Advances in Neural Information Processing Systems*, pp. 5204–5213.
- Zou, C. and Qiu, P. (2009), “Multivariate statistical process control using LASSO,” *Journal of the American Statistical Association*, 104, 1586–1596.

Appendix A: Deviation of Bayesian Inference

We slightly abuse the notation by writing

$$\tilde{\mathbf{X}}_{Z(t)} = \mathbf{X}_{Z(t)} - \mathbf{B}_{bZ(t)}\boldsymbol{\theta}_t.$$

The joint posterior distribution $p(\tilde{\mathbf{X}}, \boldsymbol{\theta}_a, \mathbf{r})$ and its logarithm transformation can be expressed as

$$\begin{aligned} p(\boldsymbol{\theta}_a, \mathbf{r}, \tilde{\mathbf{X}}_{Z(1)}, \tilde{\mathbf{X}}_{Z(2)} \dots \tilde{\mathbf{X}}_{Z(n)}) &= \prod_{t=1}^n p(\tilde{\mathbf{X}}_{Z(t)} | \boldsymbol{\theta}_a, \mathbf{r})^{\lambda_t^n} \prod_{j=1}^{k_a} p(\theta_{aj} | r_j) \prod_{j=1}^{k_a} p(r_j), \\ \ln p(\boldsymbol{\theta}_a, \mathbf{r}, \tilde{\mathbf{X}}_{Z(1)}, \tilde{\mathbf{X}}_{Z(2)} \dots \tilde{\mathbf{X}}_{Z(n)}) &= \lambda_t^n \sum_{t=1}^n \ln p(\tilde{\mathbf{X}}_{Z(t)} | \boldsymbol{\theta}_a, \mathbf{r}) + \sum_{j=1}^{k_a} \ln p(\theta_{aj} | r_j) + \sum_{j=1}^{k_a} \ln p(r_j). \end{aligned}$$

Further, the first part of $p(\tilde{\mathbf{X}}, \boldsymbol{\theta}_a, \mathbf{r})$ can be derived as

$$\begin{aligned} \prod_{t=1}^n p(\tilde{\mathbf{X}}_{Z(t)} | \boldsymbol{\theta}_a, \mathbf{r})^{\lambda_t^n} &= \prod_{t=1}^n \left(\frac{1}{(2\pi)^{p/2} \sigma_e} \exp \left(- \frac{(\tilde{\mathbf{X}}_{Z(t)} - \mathbf{B}_{aZ(t)}\boldsymbol{\theta}_a)' (\tilde{\mathbf{X}}_{Z(t)} - \mathbf{B}_{aZ(t)}\boldsymbol{\theta}_a)}{2\sigma_e^2} \right) \right)^{\lambda_t^n}, \\ \lambda_t^n \sum_{t=1}^n \ln p(\tilde{\mathbf{X}}_{Z(t)} | \boldsymbol{\theta}_a, \mathbf{r}) &= \lambda_t^n \sum_{t=1}^n \left((pc - \frac{1}{2} \ln \sigma_e^2) - \frac{1}{2\sigma_e^2} (\tilde{\mathbf{X}}'_{Z(t)} \tilde{\mathbf{X}}_{Z(t)} - 2\tilde{\mathbf{X}}'_{Z(t)} \sum_j \mathbf{B}_{ajZ(t)} \theta_{aj} \right. \\ &\quad \left. + (\sum_j \mathbf{B}_{ajZ(t)} \theta_{aj})' (\sum_j \mathbf{B}_{ajZ(t)} \theta_{aj})) \right), \end{aligned}$$

where $c = -\frac{\ln(2\pi)}{2}$. To compute negative Kullback-Leibler divergence between $p(\tilde{\mathbf{X}}, \boldsymbol{\theta}_a, \mathbf{r})$ and $q(\boldsymbol{\theta}_a, \mathbf{r})$, take its expectation under the distribution of $q(\boldsymbol{\theta}_a, \mathbf{r})$

$$\begin{aligned} E_{q(\boldsymbol{\theta}_a, \mathbf{r})} \left(\lambda_t^n \sum_{t=1}^n \ln p(\tilde{\mathbf{X}}_{Z(t)} | \boldsymbol{\theta}_a, \mathbf{r}) \right) &= (pc - \frac{1}{2} \ln \sigma_e^2) - \sum_{t=1}^n \frac{\lambda_t^n}{2\sigma_e^2} \left(\tilde{\mathbf{X}}'_{Z(t)} \tilde{\mathbf{X}}_{Z(t)} - 2\tilde{\mathbf{X}}'_{Z(t)} \sum_j \mathbf{B}_{ajZ(t)} \alpha_j \mu_{aj} \right. \\ &\quad \left. + 2 \sum_j \sum_{k \neq j} \mathbf{B}'_{ajZ(t)} \mathbf{B}_{akZ(t)} \alpha_j \alpha_k \mu_{aj} \mu_{ak} + \sum_j \mathbf{B}'_{ajZ(t)} \mathbf{B}_{ajZ(t)} ((\mu_{aj}^2 + s_j^2) \alpha_j + v s_j^2 (1 - \alpha_j)) \right). \end{aligned}$$

Also, the second part of $p(\tilde{\mathbf{X}}, \boldsymbol{\theta}_a, \mathbf{r})$ can be derived as

$$\prod_{j=1}^{k_a} p(\theta_{aj}|r_j) = \prod_{j=1}^{k_a} \left(\frac{1}{\sqrt{2\pi}\sigma_j} \exp\left(-\frac{1}{2\sigma_j^2}\theta_{aj}^2\right) \right)^{I(r_j=1)} \left(\frac{1}{\sqrt{2\pi}v\sigma_j} \exp\left(-\frac{1}{2v\sigma_j^2}\theta_{aj}^2\right) \right)^{I(r_j=0)},$$

$$\sum_{j=1}^{k_a} \ln p(\theta_{aj}|r_j) = \sum_{j=1}^{k_a} \left(\left(c - \frac{1}{2} \ln \sigma_j^2 - \frac{\theta_{aj}^2}{2\sigma_j^2}\right)r_j + \left(c - \frac{1}{2} \ln(v\sigma_j^2) - \frac{\theta_{aj}^2}{2v\sigma_j^2}\right)(1 - r_j) \right).$$

Take its expectation under the distribution of $q(\boldsymbol{\theta}_a, \mathbf{r})$

$$E_{q(\boldsymbol{\theta}_a, \mathbf{r})} \left(\sum_{j=1}^{k_a} \ln p(\theta_{aj}|r_j) \right) = \sum_{j=1}^{k_a} \left(\alpha_j \left(c - \frac{1}{2} \ln \sigma_j^2 - \frac{\mu_{aj}^2 + s_j^2}{2\sigma_j^2}\right) + (1 - \alpha_j) \left(c - \frac{1}{2} \ln(v\sigma_j^2) - \frac{vs_j^2}{2v\sigma_j^2}\right) \right).$$

And the third part of $p(\tilde{\mathbf{X}}, \boldsymbol{\theta}_a, \mathbf{r})$ can be derives as

$$\prod_{j=1}^{k_a} p(r_j) = \prod_{j=1}^{k_a} w_j^{r_j} (1 - w_j)^{1-r_j},$$

$$\sum_{j=1}^{k_a} \ln p(r_j) = \sum_{j=1}^{k_a} \left(r_j \ln(w_j) + (1 - r_j) \ln(1 - w_j) \right).$$

Take its expectation under the distribution of $q(\boldsymbol{\theta}_a, \mathbf{r})$

$$E_{q(\boldsymbol{\theta}_a, \mathbf{r})} \left(\sum_{j=1}^{k_a} \ln p(r_j) \right) = \sum_{j=1}^{k_a} \left(\alpha_j \ln(w_j) + (1 - \alpha_j) \ln(1 - w_j) \right).$$

To sum up, the expectation of joint posterior distribution $p(\tilde{\mathbf{X}}, \boldsymbol{\theta}_a, \mathbf{r})$ under the distribution of $q(\boldsymbol{\theta}_a, \mathbf{r})$ is

$$E_{q(\boldsymbol{\theta}_a, \mathbf{r})} \left(\ln p(\boldsymbol{\theta}_a, \mathbf{r}, \tilde{\mathbf{X}}_{Z(1)}, \tilde{\mathbf{X}}_{Z(2)} \dots \tilde{\mathbf{X}}_{Z(n)}) \right) = \left(pc - \frac{1}{2} \ln \sigma_e^2 \right) - \sum_{t=1}^n \frac{\lambda_t^n}{2\sigma_e^2} \left(\tilde{\mathbf{X}}'_{Z(t)} \tilde{\mathbf{X}}_{Z(t)} - 2\tilde{\mathbf{X}}'_{Z(t)} \sum_j \mathbf{B}_{ajZ(t)} \alpha_j \mu_{aj} \right)$$

$$+ 2 \sum_j \sum_{k \neq j} \mathbf{B}'_{ajZ(t)} \mathbf{B}_{akZ(t)} \alpha_j \alpha_k \mu_{aj} \mu_k + \sum_j \mathbf{B}'_{ajZ(t)} \mathbf{B}_{ajZ(t)} \left((\mu_{aj}^2 + s_j^2) \alpha_j + vs_j^2 (1 - \alpha_j) \right)$$

$$+ \sum_{j=1}^{k_a} \left(c - \frac{s_j^2}{2\sigma_j^2} + \alpha_j \left(\ln w_j - \frac{1}{2} \ln \sigma_j^2 - \frac{\mu_{aj}^2}{2\sigma_j^2} \right) + (1 - \alpha_j) \left(\ln(1 - w_j) - \frac{1}{2} \ln v\sigma_j^2 \right) \right).$$

On the other hand, the joint posterior distribution $q(\boldsymbol{\theta}_a, \mathbf{r})$ and its logarithm transformation can be expressed as

$$q(\boldsymbol{\theta}_a, \mathbf{r}) = \prod_{j=1}^{k_a} q(\theta_{aj}|r_j) \prod_{j=1}^{k_a} q(r_j),$$

$$\ln q(\boldsymbol{\theta}_a, \mathbf{r}) = \sum_{j=1}^{k_a} \ln q(\theta_{aj}|r_j) + \sum_{j=1}^{k_a} \ln q(r_j).$$

The first part of $q(\boldsymbol{\theta}_a, \mathbf{r})$ and its logarithm transformation can be derived as

$$\prod_{j=1}^{k_a} q(\theta_{aj}|r_j) = \prod_{j=1}^{k_a} \left(\frac{1}{\sqrt{2\pi}s_j} \exp\left(-\frac{(\theta_{aj} - \mu_{aj})^2}{2s_j^2}\right) \right)^{I(r_j=1)} \left(\frac{1}{\sqrt{2\pi}vs_j} \exp\left(-\frac{\theta_{aj}^2}{2vs_j^2}\right) \right)^{I(r_j=0)},$$

$$\sum_{j=1}^{k_a} \ln q(\theta_{aj}|r_j) = \sum_{j=1}^{k_a} \left(c - \frac{1}{2} \ln s_j^2 - \frac{(\theta_{aj} - \mu_{aj})^2}{2s_j^2} \right) r_j + \left(c - \frac{1}{2} \ln(vs_j^2) - \frac{\theta_{aj}^2}{2vs_j^2} \right) (1 - r_j).$$

Take its expectation under the distribution of $q(\boldsymbol{\theta}_a, \mathbf{r})$

$$E_{q(\boldsymbol{\theta}_a, \mathbf{r})} \left(\sum_{j=1}^{k_a} \ln q(\theta_{aj}|r_j) \right) = \sum_{j=1}^{k_a} \left(\left(c - \frac{1}{2} \ln s_j^2 - \frac{s_j^2}{2s_j^2} \right) \alpha_j + \left(c - \frac{1}{2} \ln(vs_j^2) - \frac{vs_j^2}{2vs_j^2} \right) (1 - \alpha_j) \right).$$

Also the second part of $q(\boldsymbol{\theta}_a, \mathbf{r})$ and its logarithm transformation can be derived as

$$\prod_{j=1}^{k_a} q(r_j) = \prod_{j=1}^{k_a} \alpha_j^{r_j} + (1 - \alpha_j)^{1-r_j},$$

$$E_{q(\boldsymbol{\theta}_a, \mathbf{r})} \left(\sum_{j=1}^{k_a} \ln q(r_j) \right) = \sum_{j=1}^{k_a} \alpha_j \ln \alpha_j + (1 - \alpha_j) \ln(1 - \alpha_j).$$

Take its expectation under the distribution of $q(\boldsymbol{\theta}_a, \mathbf{r})$

$$E_{q(\boldsymbol{\theta}_a, \mathbf{r})} \left(\ln q(\boldsymbol{\theta}_a, \mathbf{r}) \right) = \sum_{j=1}^{k_a} \left(c - \frac{1}{2} + \alpha_j (\ln \alpha_j - \frac{1}{2} \ln s_j^2) + (1 - \alpha_j) (\ln(1 - \alpha_j) - \frac{1}{2} \ln vs_j^2) \right)$$

To give a summary, the negative KL divergence between the true posterior $p(\tilde{\mathbf{X}}, \boldsymbol{\theta}_a, \mathbf{r})$ and the approximate posterior $q(\boldsymbol{\theta}_a, \mathbf{r})$ is

$$\begin{aligned}
Z &= E_{q(\boldsymbol{\theta}_a, \mathbf{r})} \left(\ln p(\boldsymbol{\theta}_a, \mathbf{r}, \tilde{\mathbf{X}}_{Z(1)}, \tilde{\mathbf{X}}_{Z(2)}, \dots, \tilde{\mathbf{X}}_{Z(n)}) \right) - E_{q(\boldsymbol{\theta}_a, \mathbf{r})} \left(\ln q(\boldsymbol{\theta}_a, \mathbf{r}) \right) \\
&= pc - \frac{1}{2} \ln \sigma_e^2 - \sum_{t=1}^n \frac{\lambda_t^n}{2\sigma_e^2} \left(\tilde{\mathbf{X}}'_{Z(t)} \tilde{\mathbf{X}}_{Z(t)} - 2\tilde{\mathbf{X}}'_{Z(t)} \sum_{j=1}^{k_a} \mathbf{B}_{ajZ(t)} \alpha_j \mu_{aj} + 2 \sum_j \sum_{k \neq j} \mathbf{B}'_{ajZ(t)} \mathbf{B}_{akZ(t)} \alpha_j \alpha_k \mu_{aj} \mu_{ak} \right. \\
&\quad \left. + \sum_{j=1}^{k_a} \mathbf{B}'_{ajZ(t)} \mathbf{B}_{ajZ(t)} ((\mu_{aj}^2 + s_j^2) \alpha_j + v s_j^2 (1 - \alpha_j)) \right) + \sum_{j=1}^{k_a} \left(\frac{1}{2} - \frac{s_j^2}{2\sigma_j^2} + \frac{1}{2} \ln \frac{s_j^2}{\sigma_j^2} + (\ln w_j - \ln \alpha_j - \frac{\mu_{aj}^2}{2\sigma_j^2}) \alpha_j \right. \\
&\quad \left. + (1 - \alpha_j)(\ln(1 - w_j) - \ln(1 - \alpha_j)) \right).
\end{aligned}$$

Taking the partial derivatives of the negative Kullback-Leibler divergence, we obtain the coordinate descent updates for this optimization problem. And let $v \rightarrow 0$, we can obtain

$$\begin{aligned}
\frac{\partial Z}{\partial s_j^2} &= - \sum_{t=1}^n \frac{\lambda_t^n}{2\sigma_e^2} \mathbf{B}'_{ajZ(t)} \mathbf{B}_{ajZ(t)} (\alpha_j + v(1 - \alpha_j)) - \frac{\alpha_j}{2\sigma_j^2} + \frac{\alpha_j}{2s_j^2} = 0 \\
s_j^2 &= \frac{1}{\sum_{t=1}^n \frac{\lambda_t^n}{\sigma_e^2} \mathbf{B}'_{ajZ(t)} \mathbf{B}_{ajZ(t)} + \frac{1}{\sigma_j^2}} \\
\frac{\partial Z}{\partial \mu_{aj}} &= - \sum_{t=1}^n \frac{\lambda_t^n}{2\sigma_e^2} (-2\tilde{\mathbf{X}}'_{Z(t)} \mathbf{B}_{ajZ(t)} \alpha_j + 2 \sum_{k \neq j} \mathbf{B}'_{ajZ(t)} \mathbf{B}_{akZ(t)} \alpha_j \alpha_k \mu_{ak} + 2\mathbf{B}'_{ajZ(t)} \mathbf{B}_{ajZ(t)} \alpha_j \mu_{aj}) - \frac{\alpha_j \mu_{aj}}{\sigma_j^2} = 0 \\
\mu_{aj} &= \frac{s_j^2}{\sigma_e^2} \sum_{t=1}^n \lambda_t^n (\tilde{\mathbf{X}}'_{Z(t)} \mathbf{B}_{ajZ(t)} - \sum_{k \neq j} \mathbf{B}'_{ajZ(t)} \mathbf{B}_{akZ(t)} \alpha_k \mu_{ak}) \\
\frac{\partial Z}{\partial \alpha_j} &= - \sum_{t=1}^n \frac{\lambda_t^n}{2\sigma_e^2} \left(-2\tilde{\mathbf{X}}'_{Z(t)} \mathbf{B}_{ajZ(t)} \mu_{aj} + 2 \sum_{k \neq j} \mathbf{B}'_{ajZ(t)} \mathbf{B}_{akZ(t)} \alpha_k \mu_{aj} \mu_{ak} + \mathbf{B}'_{ajZ(t)} \mathbf{B}_{ajZ(t)} (\mu_{aj}^2 + s_j^2 - v s_j^2) \right) \\
&\quad + \ln w_j - \frac{\mu_{aj}^2}{2\sigma_j^2} - \ln \alpha_j - \ln(1 - w_j) + \ln(1 - \alpha_j) = 0 \\
\ln \frac{\alpha_j}{1 - \alpha_j} &= \ln \frac{w_j}{1 - w_j} - \frac{\mu_{aj}^2}{2\sigma_j^2} + \mu_{aj}^2 \left(\sum_{t=1}^n \frac{\lambda_t^n}{\sigma_e^2} \mathbf{B}'_{ajZ(t)} \mathbf{B}_{ajZ(t)} + \frac{1}{\sigma_j^2} \right) - \sum_{t=1}^n \frac{\lambda_t^n}{2\sigma_e^2} \mathbf{B}'_{ajZ(t)} \mathbf{B}_{ajZ(t)} (\mu_{aj}^2 + s_j^2 - v s_j^2) \\
&= \ln \frac{w_j}{1 - w_j} + \frac{\mu_{aj}^2}{2\sigma_j^2} + \sum_{t=1}^n \frac{\lambda_t^n}{2\sigma_e^2} \mathbf{B}'_{ajZ(t)} \mathbf{B}_{ajZ(t)} (\mu_{aj}^2 - s_j^2 + v s_j^2)
\end{aligned}$$

Appendix B: Deviation of Detection Statistic

Some notations are defined as $\mathbf{A} = \mathbf{B}'_{aZ(n)}\boldsymbol{\Sigma}_e^{-1}\mathbf{B}_{aZ(n)} + \mathbf{K}^{-1}$, $\mathbf{D} = \mathbf{X}'_{Z(n)}\boldsymbol{\Sigma}_e^{-1}\mathbf{B}_{aZ(n)} + \boldsymbol{\mu}'_r\mathbf{K}^{-1}$, $\mathbf{C} = \mathbf{B}'_{bZ(n)}\boldsymbol{\Sigma}_e^{-1}\mathbf{B}_{aZ(n)}$, $\mathbf{H} = \mathbf{B}'_{bZ(n)}\boldsymbol{\Sigma}_e^{-1}\mathbf{B}_{bZ(n)} + \tilde{\boldsymbol{\Sigma}}_b^{-1}$, $\mathbf{G}^{[0]} = \mathbf{X}'_{Z(n)}\boldsymbol{\Sigma}_e^{-1}\mathbf{B}_{bZ(n)} + \tilde{\boldsymbol{\theta}}_n^{[0]'}\tilde{\boldsymbol{\Sigma}}_b^{-1}$, $\mathbf{G}^{[1]} = \mathbf{X}'_{Z(n)}\boldsymbol{\Sigma}_e^{-1}\mathbf{B}_{bZ(n)} + \tilde{\boldsymbol{\theta}}_n^{[1]'}\tilde{\boldsymbol{\Sigma}}_b^{-1}$.

The marginal likelihood under H_0 , which is the numerator of the Bayesian factor, can be derived as

$$\begin{aligned}
P(\mathbf{X}_{Z(n)}|H_0) &= \int \int p(\boldsymbol{\theta}_a|H_0)p(\boldsymbol{\theta}_n|\boldsymbol{\theta}_a, H_0)p(\mathbf{X}_{Z(n)}|\boldsymbol{\theta}_a, \boldsymbol{\theta}_n)d\boldsymbol{\theta}_nd\boldsymbol{\theta}_a \\
&= \sqrt{1/((2\pi)^{k_b+m}|\tilde{\boldsymbol{\Sigma}}_b||\boldsymbol{\Sigma}_e|)} \int \exp\left(-\frac{1}{2}\left((\boldsymbol{\theta}_n - \tilde{\boldsymbol{\theta}}_n^{[0]})'\tilde{\boldsymbol{\Sigma}}_b^{-1}(\boldsymbol{\theta}_n - \tilde{\boldsymbol{\theta}}_n) + (\mathbf{X}_{Z(n)} - \mathbf{B}_{bZ(n)}\boldsymbol{\theta}_n)'\boldsymbol{\Sigma}_e^{-1}\right.\right. \\
&\quad \left.\left.(\mathbf{X}_{Z(n)} - \mathbf{B}_{bZ(n)}\boldsymbol{\theta}_n)\right)\right)d\boldsymbol{\theta}_n \\
&= \sqrt{1/((2\pi)^{k_b+m}|\tilde{\boldsymbol{\Sigma}}_b||\boldsymbol{\Sigma}_e|)} \int \exp\left(-\frac{1}{2}\left(\boldsymbol{\theta}'_n(\tilde{\boldsymbol{\Sigma}}_b^{-1} + \mathbf{B}'_{bZ(n)}\boldsymbol{\Sigma}_e^{-1}\mathbf{B}_{bZ(n)})\boldsymbol{\theta}_n - 2(\mathbf{X}'_{Z(n)}\boldsymbol{\Sigma}_e^{-1}\mathbf{B}_{bZ(n)} + \tilde{\boldsymbol{\theta}}_n^{[0]'}\tilde{\boldsymbol{\Sigma}}_b^{-1})\right.\right. \\
&\quad \left.\left.\boldsymbol{\theta}_n + \tilde{\boldsymbol{\theta}}_n^{[0]'}\tilde{\boldsymbol{\Sigma}}_b^{-1}\tilde{\boldsymbol{\theta}}_n^{[0]} + \mathbf{X}'_{Z(n)}\boldsymbol{\Sigma}_e^{-1}\mathbf{X}_{Z(n)}\right)\right)d\boldsymbol{\theta}_n \\
&= \sqrt{1/((2\pi)^{k_b+m}|\tilde{\boldsymbol{\Sigma}}_b||\boldsymbol{\Sigma}_e|)} \exp\left(-\frac{1}{2}(\tilde{\boldsymbol{\theta}}_n^{[0]'}\tilde{\boldsymbol{\Sigma}}_b^{-1}\tilde{\boldsymbol{\theta}}_n^{[0]} + \mathbf{X}'_{Z(n)}\boldsymbol{\Sigma}_e^{-1}\mathbf{X}_{Z(n)})\right) \int \exp\left(\frac{1}{2}((\boldsymbol{\theta}_n - \mathbf{H}^{-1}\mathbf{G}^{[0]'}\mathbf{H}\right. \\
&\quad \left.(\boldsymbol{\theta}_n - \mathbf{H}^{-1}\mathbf{G}^{[0]'}) - \mathbf{G}^{[0]}\mathbf{H}^{-1}\mathbf{G}^{[0]'})\right)d\boldsymbol{\theta}_n \\
&= \sqrt{1/((2\pi)^m|\tilde{\boldsymbol{\Sigma}}_b||\boldsymbol{\Sigma}_e||\mathbf{H}|)} \exp\left(-\frac{1}{2}(\tilde{\boldsymbol{\theta}}_n^{[0]'}\tilde{\boldsymbol{\Sigma}}_b^{-1}\tilde{\boldsymbol{\theta}}_n^{[0]} + \mathbf{X}'_{Z(n)}\boldsymbol{\Sigma}_e^{-1}\mathbf{X}_{Z(n)} - \mathbf{G}^{[0]}\mathbf{H}^{-1}\mathbf{G}^{[0]'})\right).
\end{aligned}$$

The marginal likelihood under H_1 , which is the denominator of the Bayesian factor, can be

derived as

$$\begin{aligned}
P(X_{Z(n)}|H_1) &= \sum_{\mathbf{r}} \int \int p(\mathbf{r}|H_1)p(\boldsymbol{\theta}_a|\mathbf{r}, H_1)p(\boldsymbol{\theta}_n|\boldsymbol{\theta}_a, H_1)p(\mathbf{X}_{Z(n)}|\boldsymbol{\theta}_a, \boldsymbol{\theta}_n)d\boldsymbol{\theta}_nd\boldsymbol{\theta}_a \\
&= \sum_{\mathbf{r}} p(\mathbf{r}|H_1)\sqrt{1/((2\pi)^{k_a+k_b+m}|\mathbf{K}||\tilde{\Sigma}_b||\Sigma_e|)} \int \int p(\boldsymbol{\theta}_a|\mathbf{r}, H_1)p(\boldsymbol{\theta}_n|\boldsymbol{\theta}_a, H_1)p(\mathbf{X}_{Z(n)}|\boldsymbol{\theta}_a, \boldsymbol{\theta}_n)d\boldsymbol{\theta}_nd\boldsymbol{\theta}_a \\
&= \sum_{\mathbf{r}} p(\mathbf{r}|H_1)\sqrt{1/((2\pi)^{k_a+k_b+m}|\mathbf{K}||\tilde{\Sigma}_b||\Sigma_e|)} \int \int \exp\left(-\frac{1}{2}\left((\boldsymbol{\theta}_a - \boldsymbol{\mu}_r)'\mathbf{K}^{-1}(\boldsymbol{\theta}_a - \boldsymbol{\mu}_r) + (\boldsymbol{\theta}_n - \tilde{\boldsymbol{\theta}}_n)^{[1]'}\right.\right. \\
&\quad \left.\left.\tilde{\Sigma}_b^{-1}(\boldsymbol{\theta}_n - \tilde{\boldsymbol{\theta}}_n^{[1]}) + (\mathbf{X}_{Z(n)} - \mathbf{B}_{bZ(n)}\boldsymbol{\theta}_n - \mathbf{B}_{aZ(n)}\boldsymbol{\theta}_a)'\Sigma_e^{-1}(\mathbf{X}_{Z(n)} - \mathbf{B}_{bZ(n)}\boldsymbol{\theta}_n - \mathbf{B}_{aZ(n)}\boldsymbol{\theta}_a)\right)\right)d\boldsymbol{\theta}_ad\boldsymbol{\theta}_n \\
&= \sum_{\mathbf{r}} p(\mathbf{r}|H_1)\sqrt{1/((2\pi)^{k_a+k_b+m}|\mathbf{K}||\tilde{\Sigma}_b||\Sigma_e|)} \int \int \exp\left(-\frac{1}{2}\left(\boldsymbol{\theta}'_a(\mathbf{B}'_{aZ(n)}\Sigma_e^{-1}\mathbf{B}_{aZ(n)} + \mathbf{K}^{-1})\boldsymbol{\theta}_a\right.\right. \\
&\quad \left.\left.- 2((\mathbf{X}_{Z(n)} - \mathbf{B}_{bZ(n)}\boldsymbol{\theta}_n)'\Sigma_e^{-1}\mathbf{B}_{aZ(n)} + \boldsymbol{\mu}'_r\mathbf{K}^{-1})\boldsymbol{\theta}_a + \boldsymbol{\mu}'_r\mathbf{K}^{-1}\boldsymbol{\mu}_r + \boldsymbol{\theta}'_n(\mathbf{B}'_{bZ(n)}\Sigma_e^{-1}\mathbf{B}_{bZ(n)} + \tilde{\Sigma}_b^{-1})\boldsymbol{\theta}_n\right.\right. \\
&\quad \left.\left.- 2(\mathbf{X}'_{Z(n)}\Sigma_e^{-1}\mathbf{B}_{bZ(n)} + \tilde{\boldsymbol{\theta}}_n^{[1]'}\tilde{\Sigma}_b^{-1})\boldsymbol{\theta}_n + \mathbf{X}'_{Z(n)}\Sigma_e^{-1}\mathbf{X}_{Z(n)} + \tilde{\boldsymbol{\theta}}_n^{[1]'}\tilde{\Sigma}_b^{-1}\tilde{\boldsymbol{\theta}}_n^{[1]})\right)\right)d\boldsymbol{\theta}_ad\boldsymbol{\theta}_n \\
&= \sum_{\mathbf{r}} p(\mathbf{r}|H_1)\sqrt{1/((2\pi)^{k_a+k_b+m}|\mathbf{K}||\tilde{\Sigma}_b||\Sigma_e|)} \int \int \exp\left(-\frac{1}{2}\left(\boldsymbol{\theta}'_a\mathbf{A}\boldsymbol{\theta}_a - 2(\mathbf{R} - \boldsymbol{\theta}'_n\mathbf{C})\boldsymbol{\theta}_a + \boldsymbol{\theta}'_n\mathbf{H}\boldsymbol{\theta}_n\right.\right. \\
&\quad \left.\left.- 2\mathbf{G}^{[1]}\boldsymbol{\theta}_n + \boldsymbol{\mu}'_r\mathbf{K}^{-1}\boldsymbol{\mu}_r + \mathbf{X}'_{Z(n)}\Sigma_e^{-1}\mathbf{X}_{Z(n)} + \tilde{\boldsymbol{\theta}}_n^{[1]'}\tilde{\Sigma}_b^{-1}\tilde{\boldsymbol{\theta}}_n^{[1]})\right)\right)d\boldsymbol{\theta}_ad\boldsymbol{\theta}_n \\
&= \sum_{\mathbf{r}} p(\mathbf{r}|H_1)\sqrt{1/((2\pi)^{k_a+k_b+m}|\mathbf{K}||\tilde{\Sigma}_b||\Sigma_e|)} \exp\left(-\frac{1}{2}(\boldsymbol{\mu}'_r\mathbf{K}^{-1}\boldsymbol{\mu}_r + \mathbf{X}'_{Z(n)}\Sigma_e^{-1}\mathbf{X}_{Z(n)} + \tilde{\boldsymbol{\theta}}_n^{[1]'}\tilde{\Sigma}_b^{-1}\tilde{\boldsymbol{\theta}}_n^{[1]})\right) \\
&\quad \sqrt{(2\pi)^{k_a}/|\mathbf{A}|} \int \exp\left(-\frac{1}{2}(\boldsymbol{\theta}'_n(\mathbf{H} - \mathbf{C}\mathbf{A}^{-1}\mathbf{C}')\boldsymbol{\theta}_n - 2(\mathbf{G}^{[1]} - \mathbf{R}\mathbf{A}^{-1}\mathbf{C}')\boldsymbol{\theta}_n - \mathbf{R}\mathbf{A}^{-1}\mathbf{R}')\right)d\boldsymbol{\theta}_n \\
&= \sum_{\mathbf{r}} p(\mathbf{r}|H_1)\sqrt{1/((2\pi)^{k_b+m}|\mathbf{K}||\tilde{\Sigma}_b||\Sigma_e||\mathbf{A}|)} \exp\left(-\frac{1}{2}(\boldsymbol{\mu}'_r\mathbf{K}^{-1}\boldsymbol{\mu}_r + \mathbf{X}'_{Z(n)}\Sigma_e^{-1}\mathbf{X}_{Z(n)} + \tilde{\boldsymbol{\theta}}_n^{[1]'}\tilde{\Sigma}_b^{-1}\tilde{\boldsymbol{\theta}}_n^{[1]})\right) \\
&\quad \sqrt{(2\pi)^{k_b}/|\mathbf{H} - \mathbf{C}\mathbf{A}^{-1}\mathbf{C}'|} \exp\left(-\frac{1}{2}(-\mathbf{R}\mathbf{A}^{-1}\mathbf{R}' - (\mathbf{G}^{[1]} - \mathbf{R}\mathbf{A}^{-1}\mathbf{C}')(\mathbf{H} - \mathbf{C}\mathbf{A}^{-1}\mathbf{C}')^{-1}(\mathbf{G}^{[1]} - \mathbf{R}\mathbf{A}^{-1}\mathbf{C}'))\right) \\
&= \sum_{\mathbf{r}} p(\mathbf{r}|H_1)\sqrt{1/((2\pi)^m|\mathbf{K}||\tilde{\Sigma}_b||\Sigma_e||\mathbf{A}||\mathbf{H} - \mathbf{C}\mathbf{A}^{-1}\mathbf{C}'|)} \exp\left\{-\frac{1}{2}(\boldsymbol{\mu}'_r\mathbf{K}^{-1}\boldsymbol{\mu}_r + \mathbf{X}'_{Z(n)}\Sigma_e^{-1}\mathbf{X}_{Z(n)}\right. \\
&\quad \left.+ \tilde{\boldsymbol{\theta}}_n^{[1]'}\tilde{\Sigma}_b^{-1}\tilde{\boldsymbol{\theta}}_n^{[1]} - \mathbf{R}\mathbf{A}^{-1}\mathbf{R}' - (\mathbf{G}^{[1]} - \mathbf{R}\mathbf{A}^{-1}\mathbf{C}')(\mathbf{H} - \mathbf{C}\mathbf{A}^{-1}\mathbf{C}')^{-1}(\mathbf{G}^{[1]} - \mathbf{R}\mathbf{A}^{-1}\mathbf{C}'))\right\}.
\end{aligned}$$

So the posterior Bayesian factor is derived as

$$\begin{aligned}
PBF_n &= \frac{\sum_{\mathbf{r}} \int \int p(\mathbf{r}|H_1)p(\boldsymbol{\theta}_a|H_1)p(\boldsymbol{\theta}_n|\boldsymbol{\theta}_a, H_1)p(\mathbf{X}_{Z(n)}|\boldsymbol{\theta}_a, \boldsymbol{\theta}_n)d\boldsymbol{\theta}_n d\boldsymbol{\theta}_a}{\int \int p(\boldsymbol{\theta}_a|H_0)p(\boldsymbol{\theta}_n|\boldsymbol{\theta}_a, H_0)p(\mathbf{X}_{Z(n)}|\boldsymbol{\theta}_a, \boldsymbol{\theta}_n)d\boldsymbol{\theta}_n d\boldsymbol{\theta}_a} \\
&= \sum_{\mathbf{r}} p(\mathbf{r}|H_1) \sqrt{|\mathbf{H}| / (|\mathbf{K}||\mathbf{A}||\mathbf{H} - \mathbf{CA}^{-1}\mathbf{C}'|)} \exp \left(-\frac{1}{2} \left(\boldsymbol{\mu}'_r \mathbf{K}^{-1} \boldsymbol{\mu}_r + \mathbf{G}^{[0]'} \mathbf{H}^{-1} \mathbf{G}^{[0]} - \mathbf{RA}^{-1} \mathbf{R}' \right. \right. \\
&\quad \left. \left. - (\mathbf{G}^{[1]} - \mathbf{RA}^{-1} \mathbf{C}') (\mathbf{H} - \mathbf{CA}^{-1} \mathbf{C}')^{-1} (\mathbf{G}^{[1]} - \mathbf{RA}^{-1} \mathbf{C}')' + \tilde{\boldsymbol{\theta}}_n^{[1]'} \tilde{\boldsymbol{\Sigma}}_b^{-1} \tilde{\boldsymbol{\theta}}_n^{[1]} - \tilde{\boldsymbol{\theta}}_n^{[0]'} \tilde{\boldsymbol{\Sigma}}_b^{-1} \tilde{\boldsymbol{\theta}}_n^{[0]} \right) \right).
\end{aligned}$$

Note that the form of PBF_n is too complex for easy computation. We consider further simplifying it by eliminating constants and small values as below.

For a square matrix \mathbf{M} with spectral radius $\rho(\mathbf{M}) < 1$, according to the Maclaurin series of matrix form, $(\mathbf{I} + \mathbf{M})^{-1} = \sum_{k=0}^{\infty} (-1)^k \mathbf{M}^k$. Since $\mathbf{K} \frac{\mathbf{B}'_{aZ(n)} \mathbf{B}_{aZ(n)}}{\sigma_e^2}$ is a square matrix and the entries of \mathbf{K} are quite small, the spectral radius $\rho(\mathbf{K} \frac{\mathbf{B}'_{aZ(n)} \mathbf{B}_{aZ(n)}}{\sigma_e^2}) \leq \|\mathbf{K} \frac{\mathbf{B}'_{aZ(n)} \mathbf{B}_{aZ(n)}}{\sigma_e^2}\| < 1$ can be satisfied. Then we can generalize it as

$$\mathbf{A}^{-1} = \left(\frac{\mathbf{B}'_{aZ(n)} \mathbf{B}_{aZ(n)}}{\sigma_e^2} + \mathbf{K}^{-1} \right)^{-1} = \sum_{k=0}^{\infty} (-1)^k \left(\mathbf{K} \frac{\mathbf{B}'_{aZ(n)} \mathbf{B}_{aZ(n)}}{\sigma_e^2} \right)^k \mathbf{K} \approx \mathbf{K} - \mathbf{K} \frac{\mathbf{B}'_{aZ(n)} \mathbf{B}_{aZ(n)}}{\sigma_e^2} \mathbf{K} + o(\mathbf{K}^2).$$

Following the same way, consider $\mathbf{H}^{-1} \mathbf{CA}^{-1} \mathbf{C}'$ is a square matrix and the entries of \mathbf{H}^{-1} are quite small. The spectral radius $\rho(\mathbf{H}^{-1} \mathbf{CA}^{-1} \mathbf{C}') \leq \|\mathbf{H}^{-1} \mathbf{CA}^{-1} \mathbf{C}'\| < 1$ can be satisfied as well. Then,

$$(\mathbf{H} - \mathbf{CA}^{-1} \mathbf{C}')^{-1} = \mathbf{H}^{-1} + \mathbf{H}^{-1} \mathbf{CA}^{-1} \mathbf{C}' \mathbf{H}^{-1} + o((\mathbf{H}^{-1})^2).$$

Then the following items can be simplified as

$$\begin{aligned}
& (\mathbf{G}^{[1]} - \mathbf{R}\mathbf{A}^{-1}\mathbf{C}')(\mathbf{H} - \mathbf{C}\mathbf{A}^{-1}\mathbf{C}')^{-1}(\mathbf{G}^{[1]} - \mathbf{R}\mathbf{A}^{-1}\mathbf{C}')' = (\mathbf{G}^{[1]} - \mathbf{R}\mathbf{A}^{-1}\mathbf{C}')\mathbf{H}^{-1}(\mathbf{G}^{[1]} - \mathbf{R}\mathbf{A}^{-1}\mathbf{C}')' \\
& + (\mathbf{G}^{[1]} - \mathbf{R}\mathbf{A}^{-1}\mathbf{C}')\mathbf{H}^{-1}\mathbf{C}\mathbf{A}^{-1}\mathbf{C}'\mathbf{H}^{-1}(\mathbf{G}^{[1]} - \mathbf{R}\mathbf{A}^{-1}\mathbf{C}')' \\
& = \mathbf{G}^{[1]}\mathbf{H}^{-1}\mathbf{G}^{[1]'} + (\mathbf{R}\mathbf{A}^{-1}\mathbf{C}')\mathbf{H}^{-1}(\mathbf{R}\mathbf{A}^{-1}\mathbf{C}')' - 2\mathbf{R}\mathbf{A}^{-1}\mathbf{C}'\mathbf{H}^{-1}\mathbf{G}^{[1]}' \\
\mathbf{R}\mathbf{A}^{-1}\mathbf{C}' & = \left(\frac{\mathbf{X}'_{Z(n)}\mathbf{B}_{aZ(n)}}{\sigma_e^2} + \boldsymbol{\mu}'_r\mathbf{K}^{-1} \right) \mathbf{K} \frac{\mathbf{B}'_{aZ(n)}\mathbf{B}_{bZ(n)}}{\sigma_e^2} = \frac{\mathbf{X}'_{Z(n)}\mathbf{B}_{aZ(n)}}{\sigma_e^2} \mathbf{K} \frac{\mathbf{B}'_{aZ(n)}\mathbf{B}_{bZ(n)}}{\sigma_e^2} + \boldsymbol{\mu}'_r \frac{\mathbf{B}'_{aZ(n)}\mathbf{B}_{bZ(n)}}{\sigma_e^2}. \\
\mathbf{R}\mathbf{A}^{-1}\mathbf{R}' & = \left(\frac{\mathbf{X}'_{Z(n)}\mathbf{B}_{aZ(n)}}{\sigma_e^2} + \boldsymbol{\mu}'_r\mathbf{K}^{-1} \right) (\mathbf{K} - \mathbf{K} \frac{\mathbf{B}'_{aZ(n)}\mathbf{B}_{aZ(n)}}{\sigma_e^2} \mathbf{K}) \left(\frac{\mathbf{X}'_{Z(n)}\mathbf{B}_{aZ(n)}}{\sigma_e^2} + \boldsymbol{\mu}'_r\mathbf{K}^{-1} \right)' \\
& = \frac{\mathbf{X}'_{Z(n)}\mathbf{B}_{aZ(n)}}{\sigma_e^2} \mathbf{K} \frac{\mathbf{B}'_{aZ(n)}\mathbf{X}_{Z(n)}}{\sigma_e^2} + \boldsymbol{\mu}'_r\mathbf{K}^{-1}\boldsymbol{\mu}_r + 2 \frac{\mathbf{X}'_{Z(n)}\mathbf{B}_{aZ(n)}}{\sigma_e^2} \boldsymbol{\mu}_r - \boldsymbol{\mu}'_r \frac{\mathbf{B}'_{aZ(n)}\mathbf{B}_{aZ(n)}}{\sigma_e^2} \boldsymbol{\mu}_r \\
& - 2\boldsymbol{\mu}'_r \frac{\mathbf{B}'_{aZ(n)}\mathbf{B}_{aZ(n)}}{\sigma_e^2} \mathbf{K} \frac{\mathbf{B}'_{aZ(n)}\mathbf{X}_{Z(n)}}{\sigma_e^2} \\
& = \boldsymbol{\mu}'_r\mathbf{K}^{-1}\boldsymbol{\mu}_r + 2 \frac{\mathbf{X}'_{Z(n)}\mathbf{B}_{aZ(n)}}{\sigma_e^2} \boldsymbol{\mu}_r - \boldsymbol{\mu}'_r \frac{\mathbf{B}'_{aZ(n)}\mathbf{B}_{aZ(n)}}{\sigma_e^2} \boldsymbol{\mu}_r + o(\mathbf{K}).
\end{aligned}$$

Similarly, consider $\tilde{\boldsymbol{\Sigma}}_b \frac{\mathbf{B}_{bZ(n)}'\mathbf{B}_{bZ(n)}}{\sigma_e^2}$ is a square matrix and the entries of $\tilde{\boldsymbol{\Sigma}}_b$ are quite small. Its spectral radius $\rho(\tilde{\boldsymbol{\Sigma}}_b \frac{\mathbf{B}_{bZ(n)}'\mathbf{B}_{bZ(n)}}{\sigma_e^2}) \leq \|\tilde{\boldsymbol{\Sigma}}_b \frac{\mathbf{B}_{bZ(n)}'\mathbf{B}_{bZ(n)}}{\sigma_e^2}\| < 1$ can be satisfied. Then,

$$\begin{aligned}
\mathbf{H}^{-1} & = \left(\frac{\mathbf{B}_{bZ(n)}'\mathbf{B}_{bZ(n)}}{\sigma_e^2} + \tilde{\boldsymbol{\Sigma}}_b^{-1} \right)^{-1} = \tilde{\boldsymbol{\Sigma}}_b - \tilde{\boldsymbol{\Sigma}}_b \frac{\mathbf{B}_{bZ(n)}'\mathbf{B}_{bZ(n)}}{\sigma_e^2} \tilde{\boldsymbol{\Sigma}}_b + \tilde{\boldsymbol{\Sigma}}_b \frac{\mathbf{B}'_{bZ(n)}\mathbf{B}_{bZ(n)}}{\sigma_e^2} \tilde{\boldsymbol{\Sigma}}_b \frac{\mathbf{B}_{bZ(n)}'\mathbf{B}_{bZ(n)}}{\sigma_e^2} \tilde{\boldsymbol{\Sigma}}_b \\
& + o(\tilde{\boldsymbol{\Sigma}}_b^2). \\
\mathbf{H}^{-1}\mathbf{G}^{[1]'} & = (\tilde{\boldsymbol{\Sigma}}_b - \tilde{\boldsymbol{\Sigma}}_b \frac{\mathbf{B}_{bZ(n)}'\mathbf{B}_{bZ(n)}}{\sigma_e^2} \tilde{\boldsymbol{\Sigma}}_b) (\tilde{\boldsymbol{\Sigma}}_b^{-1} \tilde{\boldsymbol{\theta}}_n^{[1]} + \frac{\mathbf{B}_{bZ(n)}'\mathbf{X}_{Z(n)}}{\sigma_e^2}) \\
& = \tilde{\boldsymbol{\theta}}_n^{[1]} - \tilde{\boldsymbol{\Sigma}}_b \frac{\mathbf{B}'_{bZ(n)}\mathbf{B}_{bZ(n)}}{\sigma_e^2} \tilde{\boldsymbol{\theta}}_n^{[1]} - \tilde{\boldsymbol{\Sigma}}_b \frac{\mathbf{B}_{bZ(n)}'\mathbf{B}_{bZ(n)}}{\sigma_e^2} \tilde{\boldsymbol{\Sigma}}_b \frac{\mathbf{B}'_{bZ(n)}\mathbf{X}_{Z(n)}}{\sigma_e^2} + \tilde{\boldsymbol{\Sigma}}_b \frac{\mathbf{B}'_{bZ(n)}\mathbf{X}_{Z(n)}}{\sigma_e^2}. \\
\mathbf{R}\mathbf{A}^{-1}\mathbf{C}'\mathbf{H}^{-1}\mathbf{G}' & = \boldsymbol{\mu}'_r \frac{\mathbf{B}'_{aZ(n)}\mathbf{B}_{aZ(n)}}{\sigma_e^2} \tilde{\boldsymbol{\theta}}_n^{[1]} - \boldsymbol{\mu}'_r \frac{\mathbf{B}'_{aZ(n)}\mathbf{B}_{bZ(n)}}{\sigma_e^2} \tilde{\boldsymbol{\Sigma}}_b \frac{\mathbf{B}'_{bZ(n)}\mathbf{B}_{bZ(n)}}{\sigma_e^2} \tilde{\boldsymbol{\theta}}_n^{[1]} \\
& - \boldsymbol{\mu}'_r \frac{\mathbf{B}'_{aZ(n)}\mathbf{B}_{bZ(n)}}{\sigma_e^2} \tilde{\boldsymbol{\Sigma}}_b \frac{\mathbf{B}'_{bZ(n)}\mathbf{B}_{bZ(n)}}{\sigma_e^2} \tilde{\boldsymbol{\Sigma}}_b \frac{\mathbf{B}'_{bZ(n)}\mathbf{X}_{Z(n)}}{\sigma_e^2} + \boldsymbol{\mu}'_r \frac{\mathbf{B}'_{aZ(n)}\mathbf{B}_{bZ(n)}}{\sigma_e^2} \tilde{\boldsymbol{\Sigma}}_b \frac{\mathbf{B}'_{bZ(n)}\mathbf{X}_{Z(n)}}{\sigma_e^2}. \\
\mathbf{R}\mathbf{A}^{-1}\mathbf{C}'\mathbf{H}^{-1}(\mathbf{R}\mathbf{A}^{-1}\mathbf{C}')' & = \boldsymbol{\mu}'_r \frac{\mathbf{B}'_{aZ(n)}\mathbf{B}_{bZ(n)}}{\sigma_e^2} \tilde{\boldsymbol{\Sigma}}_b \frac{\mathbf{B}'_{bZ(n)}\mathbf{B}_{aZ(n)}}{\sigma_e^2} \boldsymbol{\mu}_r - \boldsymbol{\mu}'_r \frac{\mathbf{B}'_{aZ(n)}\mathbf{B}_{bZ(n)}}{\sigma_e^2} \tilde{\boldsymbol{\Sigma}}_b \frac{\mathbf{B}'_{bZ(n)}\mathbf{B}_{bZ(n)}}{\sigma_e^2} \\
& \tilde{\boldsymbol{\Sigma}}_b \frac{\mathbf{B}'_{bZ(n)}\mathbf{B}_{aZ(n)}}{\sigma_e^2} \boldsymbol{\mu}_r.
\end{aligned}$$

So the terms inside the exponential function in PBF_n is simplified as

$$\begin{aligned}
& \boldsymbol{\mu}'_r \mathbf{K}^{-1} \boldsymbol{\mu}_r + \mathbf{G}^{[0]} \mathbf{H}^{-1} \mathbf{G}^{[0]'} - \mathbf{R} \mathbf{A}^{-1} \mathbf{R}' - (\mathbf{G}^{[1]} - \mathbf{R} \mathbf{A}^{-1} \mathbf{C}') (\mathbf{H} - \mathbf{C} \mathbf{A}^{-1} \mathbf{C}')^{-1} (\mathbf{G}^{[1]} - \mathbf{R} \mathbf{A}^{-1} \mathbf{C}')' \\
& + \tilde{\boldsymbol{\theta}}_n^{[1]'} \tilde{\boldsymbol{\Sigma}}_b^{-1} \tilde{\boldsymbol{\theta}}_n^{[1]} - \tilde{\boldsymbol{\theta}}_n^{[0]'} \tilde{\boldsymbol{\Sigma}}_b^{-1} \tilde{\boldsymbol{\theta}}_n^{[0]} \\
& = \boldsymbol{\mu}'_r \mathbf{K}^{-1} \boldsymbol{\mu}_r + \mathbf{G}^{[0]} \mathbf{H}^{-1} \mathbf{G}^{[0]'} - \mathbf{R} \mathbf{A}^{-1} \mathbf{R}' - \mathbf{G}^{[1]} \mathbf{H}^{-1} \mathbf{G}^{[1]'} - (\mathbf{R} \mathbf{A}^{-1} \mathbf{C}') \mathbf{H}^{-1} (\mathbf{R} \mathbf{A}^{-1} \mathbf{C}')' \\
& + 2 \mathbf{R} \mathbf{A}^{-1} \mathbf{C}' \mathbf{H}^{-1} \mathbf{G}^{[1]'} + \tilde{\boldsymbol{\theta}}_n^{[1]'} \tilde{\boldsymbol{\Sigma}}_b^{-1} \tilde{\boldsymbol{\theta}}_n^{[1]} - \tilde{\boldsymbol{\theta}}_n^{[0]'} \tilde{\boldsymbol{\Sigma}}_b^{-1} \tilde{\boldsymbol{\theta}}_n^{[0]} \\
& = 2 \frac{\mathbf{X}'_{Z(n)} \mathbf{B}_{bZ(n)}}{\sigma_e^2} \tilde{\boldsymbol{\Sigma}}_b \frac{\mathbf{B}'_{bZ(n)} \mathbf{B}_{aZ(n)}}{\sigma_e^2} \tilde{\boldsymbol{\mu}}_a - \tilde{\boldsymbol{\mu}}_a' \frac{\mathbf{B}'_{aZ(n)} \mathbf{B}_{bZ(n)}}{\sigma_e^2} \tilde{\boldsymbol{\Sigma}}_b \frac{\mathbf{B}'_{bZ(n)} \mathbf{B}_{bZ(n)}}{\sigma_e^2} \tilde{\boldsymbol{\Sigma}}_b \frac{\mathbf{B}'_{bZ(n)} \mathbf{B}_{aZ(n)}}{\sigma_e^2} \tilde{\boldsymbol{\mu}}_a \\
& - 2 \frac{\mathbf{X}'_{Z(n)} \mathbf{B}_{aZ(n)}}{\sigma_e^2} \boldsymbol{\mu}_r + \boldsymbol{\mu}'_r \frac{\mathbf{B}'_{aZ(n)} \mathbf{B}_{aZ(n)}}{\sigma_e^2} \boldsymbol{\mu}_r - \boldsymbol{\mu}'_r \frac{\mathbf{B}'_{aZ(n)} \mathbf{B}_{bZ(n)}}{\sigma_e^2} \tilde{\boldsymbol{\Sigma}}_b \frac{\mathbf{B}'_{bZ(n)} \mathbf{B}_{aZ(n)}}{\sigma_e^2} \boldsymbol{\mu}_r \\
& + \boldsymbol{\mu}'_r \frac{\mathbf{B}'_{aZ(n)} \mathbf{B}_{bZ(n)}}{\sigma_e^2} \tilde{\boldsymbol{\Sigma}}_b \frac{\mathbf{B}'_{bZ(n)} \mathbf{B}_{bZ(n)}}{\sigma_e^2} \tilde{\boldsymbol{\Sigma}}_b \frac{\mathbf{B}'_{bZ(n)} \mathbf{B}_{aZ(n)}}{\sigma_e^2} \boldsymbol{\mu}_r + 2 \boldsymbol{\mu}'_r \frac{\mathbf{B}'_{aZ(n)} \mathbf{B}_{bZ(n)}}{\sigma_e^2} \tilde{\boldsymbol{\theta}}_n^{[1]} \\
& - 2 \boldsymbol{\mu}'_r \frac{\mathbf{B}'_{aZ(n)} \mathbf{B}_{bZ(n)}}{\sigma_e^2} \tilde{\boldsymbol{\Sigma}}_b \frac{\mathbf{B}'_{bZ(n)} \mathbf{B}_{bZ(n)}}{\sigma_e^2} \tilde{\boldsymbol{\theta}}_n^{[1]} + 2 \boldsymbol{\mu}'_r \frac{\mathbf{B}'_{aZ(n)} \mathbf{B}_{bZ(n)}}{\sigma_e^2} \tilde{\boldsymbol{\Sigma}}_b \frac{\mathbf{B}'_{bZ(n)} \mathbf{X}_{Z(n)}}{\sigma_e^2} \\
& - 2 \boldsymbol{\mu}'_r \frac{\mathbf{B}'_{aZ(n)} \mathbf{B}_{bZ(n)}}{\sigma_e^2} \tilde{\boldsymbol{\Sigma}}_b \frac{\mathbf{B}'_{bZ(n)} \mathbf{B}_{bZ(n)}}{\sigma_e^2} \tilde{\boldsymbol{\Sigma}}_b \frac{\mathbf{B}'_{aZ(n)} \mathbf{X}_{Z(n)}}{\sigma_e^2} \\
& = -2 \boldsymbol{\mu}'_r \frac{\mathbf{B}'_{aZ(n)}}{\sigma_e^2} (\mathbf{X}_{Z(n)} - \mathbf{B}_{bZ(n)} \tilde{\boldsymbol{\theta}}_n^{[1]}) + \boldsymbol{\mu}'_r \frac{\mathbf{B}'_{aZ(n)} \mathbf{B}_{aZ(n)}}{\sigma_e^2} \boldsymbol{\mu}_r + 2 \tilde{\boldsymbol{\mu}}_a' \frac{\mathbf{B}'_{aZ(n)}}{\sigma_e^2} \hat{\mathbf{H}} \mathbf{X}_{Z(n)} - 2 \boldsymbol{\mu}'_r \frac{\mathbf{B}'_{aZ(n)}}{\sigma_e^2} \hat{\mathbf{H}} \mathbf{B}_{bZ(n)} \tilde{\boldsymbol{\theta}}_n^{[1]} \\
& - \tilde{\boldsymbol{\mu}}_a' \frac{\mathbf{B}'_{aZ(n)}}{\sigma_e^2} \mathbf{B}_{aZ(n)} \tilde{\boldsymbol{\mu}}_a,
\end{aligned}$$

where $\hat{\mathbf{H}} = \mathbf{B}_{bZ(n)} (\mathbf{B}'_{bZ(n)} \mathbf{B}_{bZ(n)})^{-1} \mathbf{B}'_{bZ(n)}$. Since $\mathbf{C} \mathbf{A}^{-1} \mathbf{C}'$ is quite small and $\mathbf{A}^{-1} \approx \mathbf{K}$, $\sqrt{|\mathbf{H}|/|\mathbf{K}| |\mathbf{A}| |\mathbf{H} - \mathbf{C} \mathbf{A}^{-1} \mathbf{C}'|} \approx 1$, we drop this constant term. Furthermore, we consider Taylor expansion on each exponential term of Λ_n , i.e., $\exp(x) = 1 + x + x^2/2! + x^3/3! + \dots$ for further simplification. Consider under H_0 , the term inside the exponential function is usually very close to zero. The first-order expansion would be a sufficient approximation. So the detection statistic can be defined as

$$\Lambda_n \equiv 2 \tilde{\boldsymbol{\mu}}_a' \mathbf{B}'_{aZ(n)} (\mathbf{I} - \hat{\mathbf{H}}) (\mathbf{X}_{Z(n)} - \mathbf{B}_{bZ(n)} \tilde{\boldsymbol{\theta}}_n^{[1]}) - \boldsymbol{\mu}'_a (\mathbf{B}'_{aZ(n)} \mathbf{B}_{aZ(n)} \circ \bar{\mathbf{A}}) \boldsymbol{\mu}_a + \tilde{\boldsymbol{\mu}}_a' \mathbf{B}'_{aZ(n)} \hat{\mathbf{H}} \mathbf{B}_{aZ(n)} \tilde{\boldsymbol{\mu}}_a,$$

where $\bar{\mathbf{A}}$ has diagonal items $\bar{A}_{ii} = \alpha_i, i = 1, \dots, k_a$, and other items $\bar{A}_{ij} = \alpha_i \alpha_j, \forall i, j = 1, \dots, k_a, i \neq j$.

Appendix C: Verification of Subspace Orthogonal Property

For a vector $\mathbf{b} \in \mathbb{R}^p$ with $\|\mathbf{b}\|_2^2 = 1$, denote $\mathbf{b}^2 = (b_1^2, b_2^2, \dots, b_p^2)'$ and assume that $\|\mathbf{b}^2\|_\infty \leq \frac{c}{p}\|\mathbf{b}\|_2^2$, where $1 \leq c \leq p$. Consider \mathbf{P} is subspace projection matrix from $\mathbb{R}^p \mapsto \mathbb{R}^m$, where m out of p dimensions have $P_{ii} = 1$, and all other entries of \mathbf{P} have values of 0. Without loss of generality, we can assume that $E[P_{ii}] \geq E[P_{jj}]$ for any $i \leq j$. Thus, $E[\mathbf{P}] = \tilde{\mathbf{P}} = \text{diag}\{a_1, a_2, \dots, a_p\}$, where $0 \leq a_p \leq a_{p-1} \leq \dots \leq a_1 \leq 1$ and $\sum_{i=1}^p a_i = m$. Then we have

$$a_p \|\mathbf{b}\|_2^2 \leq E[\|\mathbf{P}\mathbf{b}\|_2^2] = \tilde{\mathbf{P}}\|\mathbf{b}\|_2^2 \leq a_1 \|\mathbf{b}\|_2^2.$$

Following [Hoeffding \(1994\)](#); [Dasgupta and Gupta \(1999\)](#), we have the one side

$$\begin{aligned} Pr\left\{\frac{1}{a_1}\|\mathbf{P}\mathbf{b}\|_2^2 - \|\mathbf{b}\|_2^2 \geq \epsilon\right\} &\leq Pr\left\{\frac{1}{a_1}\|\mathbf{P}\mathbf{b}\|_2^2 - \frac{1}{a_1}E[\|\mathbf{P}\mathbf{b}\|_2^2] \geq \epsilon\right\} \leq \exp\left(-\frac{2a_1^2\epsilon^2}{m\|\mathbf{b}^2\|_\infty^2}\right) \\ &\leq \exp\left(-\frac{2a_1^2p^2\epsilon^2}{mc^2}\right) \leq \exp\left(-\frac{2\left(\frac{m}{p}\right)^2p^2\epsilon^2}{mc^2}\right) = \exp\left(-\frac{2m\epsilon^2}{c^2}\right), \end{aligned}$$

and the other side

$$\begin{aligned} Pr\left\{\|\mathbf{b}\|_2^2 - \frac{1}{a_p}\|\mathbf{P}\mathbf{b}\|_2^2 \geq \epsilon\right\} &\leq Pr\left\{\frac{1}{a_p}E[\|\mathbf{P}\mathbf{b}\|_2^2] - \frac{1}{a_p}\|\mathbf{P}\mathbf{b}\|_2^2 \geq \epsilon\right\} \leq \exp\left(-\frac{2a_p^2\epsilon^2}{m\|\mathbf{b}^2\|_\infty^2}\right) \\ &\leq \exp\left(-\frac{2a_p^2p^2\epsilon^2}{mc^2}\right). \end{aligned}$$

Now in our scenario, assume \mathbf{B}_a and \mathbf{B}_b are two orthogonal spaces, i.e., $\mathbf{B}'_a\mathbf{B}_b = \mathbf{0}$. We set \mathbf{b} as $\frac{\mathbf{b}_{ai} - \mathbf{b}_{bj}}{\|\mathbf{b}_{ai} - \mathbf{b}_{bj}\|}$, where \mathbf{b}_{ai} and \mathbf{b}_{bj} are any column of \mathbf{B}_a and \mathbf{B}_b respectively. Then with probability $1 - \delta$,

$$\begin{aligned} \frac{1}{a_1}\|\mathbf{P}(\mathbf{b}_{ai} - \mathbf{b}_{bj})\|_2^2 &\leq (1 + \epsilon)\|\mathbf{b}_{ai} - \mathbf{b}_{bj}\|_2^2, \\ \frac{1}{a_p}\|\mathbf{P}(\mathbf{b}_{ai} - \mathbf{b}_{bj})\|_2^2 &\geq (1 - \epsilon)\|\mathbf{b}_{ai} - \mathbf{b}_{bj}\|_2^2. \end{aligned}$$

With probability $1 - 2\delta$, we also have

$$a_p(\mathbf{b}'_{ai}\mathbf{b}_{bj} - \epsilon\|\mathbf{b}_{ai}\|_2\|\mathbf{b}_{bj}\|_2) \leq \mathbf{b}'_{aiZ}\mathbf{b}_{bjZ} \leq a_1(\mathbf{b}'_{ai}\mathbf{b}_{bj} + \epsilon\|\mathbf{b}_{ai}\|_2\|\mathbf{b}_{bj}\|_2)$$

From the foregoing two-side constraints, we can obtain that when $\frac{c^2}{2\epsilon^2}\log(\frac{(k_a+k_b)^2}{\delta}) \leq m \leq \frac{2a_p^2p^2\epsilon^2}{c^2\log(\frac{(k_a+k_b)^2}{\delta})}$, $-a_p\epsilon \leq \mathbf{b}'_{aiZ}\mathbf{b}_{bjZ} \leq a_1\epsilon$ holds with probability $1 - 2\delta$, where $0 \leq a_p \leq a_1 \leq 1$. So we can verify that the subspaces of \mathbf{B}_a and \mathbf{B}_b are approximately orthogonal when m satisfies the foregoing conditions.

Appendix D: Proof of Theorem 1 and Theorem 2

The simplified sampling procedure is to sample Z by ranking $\Lambda_{(n+1)i} = \left(2\hat{\mathbf{X}}_1'\mathbf{B}'_{ai}\mathbf{B}_{ai}\tilde{\boldsymbol{\mu}}_a - \boldsymbol{\mu}'_a(\mathbf{B}'_{ai}\mathbf{B}_{ai}\circ\bar{\mathbf{A}})\boldsymbol{\mu}_a\right)$, $i = 1, \dots, p$ from the largest to the smallest and select the top m variables. $\hat{\mathbf{X}}_1$ is generated by sampling $\hat{\boldsymbol{\theta}}_a$ from $\tilde{p}(\boldsymbol{\theta}_a, \mathbf{r})$, sampling $\hat{\mathbf{E}}$ from $N(\mathbf{0}, \boldsymbol{\Sigma}_e)$ and getting $\hat{\mathbf{X}}_1 = \mathbf{B}_a\hat{\boldsymbol{\theta}}_a + \hat{\mathbf{E}}$.

Since the posterior distribution of $\boldsymbol{\theta}_a$ is in spike-slab form, the distribution of $\Lambda_{(n+1)i}$ is Gaussian mixture distribution, which means it follows 2^{k_a} Gaussian distribution, each with different probability. If denote $S = \{1, 2, \dots, k_a\}$, for any subset S_0 of S , we have

$$\Lambda_i \sim N\left(2 \sum_{j \in S \setminus S_0} B_{aij}\mu_{aj} \sum_{k \in S} B_{aik}\mu_{ak}\alpha_k - \sum_{j \in S} B_{aij}^2\mu_{aj}^2\alpha_j - 2 \sum_{\forall j_1, j_2 \in S, j_1 \neq j_2} B_{aij_1}B_{aij_2}\mu_{aj_1}\mu_{aj_2}\alpha_{j_1}\alpha_{j_2}, \right. \\ \left. 4\left(\sum_{j \in S \setminus S_0} B_{aij}^2s_j^2 + \sum_{j \in S_0} B_{aij}^2vs_j^2 + \sigma_e^2\right)\left(\sum_{j \in S} B_{aij}\mu_{aj}\alpha_j\right)^2\right)$$

with probability $\prod_{j \in S \setminus S_0} \alpha_j \prod_{j \in S_0} (1 - \alpha_j)$.

According to Theorem 5 of [Wang and Blei \(2019\)](#), the VB posterior converges to point mass of the true parameter value in distribution. Under our case, in normal condition, the true value of θ_{aj} equals 0, $\forall j = 1 \dots k_a$. The posterior distribution that we obtain through VB method is in spike-slab form. For example, $q_j(\theta_{aj}) \sim N(\mu_{aj}, s_j^2)$ with probability α_j and

$q_j(\theta_{aj}) \sim N(0, vs_j^2)$ with probability $1 - \alpha_j$. Then suggested by Theorem 5 of Wang and Blei (2019), as $n \rightarrow \infty$,

$$q_j(\theta_{aj}) \xrightarrow{d} \delta_0, \forall j, \quad (24)$$

where δ_0 is a point mass at 0. That suggests $\mu_{aj} \rightarrow 0$ and $s_j^2 \rightarrow 0$. So in normal condition, $E(\Lambda_{(n+1)i}) \rightarrow 0$ and $Var(\Lambda_{(n+1)i}) \rightarrow 0, \forall j = 1 \dots k_a$, which means under the limit conditions, we sample the variables $Z(n+1)$ randomly.

Following a similar way, in abnormal condition, assume the anomaly relates to certain bases $\mathcal{A} \subset S$. For $l \in \mathcal{A}$, assume the anomaly relates to the l^{th} base has change magnitude ϕ_l . Then suggested by Theorem 5 of Wang and Blei (2019), as $n \rightarrow \infty$,

$$q_l(\theta_{al}) \xrightarrow{d} \delta_{\phi_l}, \forall l \in \mathcal{A} \quad (25)$$

$$q_j(\theta_{aj}) \xrightarrow{d} \delta_0, \forall j \in S - \mathcal{A} \quad (26)$$

where δ_{ϕ_l} is a point mass at ϕ_l . That suggests $\mu_{al} \rightarrow \phi_l, \alpha_l \rightarrow 1$ and $s_l^2 \rightarrow 0$. The same as normal condition, $\mu_{aj} \rightarrow 0$ and $s_j^2 \rightarrow 0, \forall j \neq l$. So in abnormal condition, $E(\Lambda_{(n+1)i}) \rightarrow \sum_{l \in \mathcal{A}} B_{ail}^2 \phi_l^2 + 2 \sum_{l_1, l_2 \in \mathcal{A}, l_1 \neq l_2} B_{ail_1} B_{ail_2} \phi_{l_1} \phi_{l_2}$ and $Var(\Lambda_{(n+1)i}) \rightarrow 0, \forall j = 1 \dots k_a$. Similar proof can be extended to cases when anomaly relates to multiple bases.

For general cases with $\theta_n \mathbf{B}_n$, When $m \rightarrow \infty$ and $p \rightarrow \infty$ but the fraction $\frac{m}{p} \rightarrow \eta$, with η being an arbitrary number between 0 and 1, according to the consistency of posterior estimation in Bayesian theory (Ghosh et al. 2007), $\tilde{\theta}_n \rightarrow \theta_n$. Then the properties of θ_a in (24) and (25) still hold. Consequently, Theorem 1 and Theorem 2 hold.

Appendix E: Simulation Results for 1D and 2D Cases

Table 2: Average Detection Delays/ADDs(Standard Deviation of Detection Delays/STDs) for 1D data with $m = 10$

ϕ	TRAS	CMAB(s)	NAS	SASAM	CDSSD	CDSSD(I)	ORACLE
0.0	200(142)	200(180)	200(221)	200(111)	200(266)	200(250)	200(361)
0.1	163(102)	33.6(19.8)	192(212)	170(96.5)	15.2 (18.0)	20.4(22.8)	2.90(2.60)
0.2	133(89.8)	14.5(6.96)	161(176)	115(61.6)	4.68 (3.67)	5.12(4.07)	1.30(0.55)
0.3	109(77.6)	9.78(5.03)	151(166)	74.5(39.4)	2.85(2.22)	2.84 (2.24)	1.05(0.24)
0.4	98.0(76.0)	7.70(4.66)	136(148)	52.6(27.1)	2.26(1.63)	2.13 (1.60)	1.00(0.08)
0.5	86.0(70.0)	6.39(4.06)	141(157)	38.5(19.5)	2.00(1.50)	1.73 (1.43)	1.00(0.00)
0.6	77.8(67.9)	5.46(3.56)	135(151)	31.1(15.8)	1.77(1.31)	1.64 (1.21)	1.00(0.00)
0.7	74.2(69.0)	4.86(3.73)	130(143)	26.5(13.5)	1.63(1.07)	1.54 (1.14)	1.00(0.00)
0.8	71.1(69.3)	4.18(3.31)	135(149)	22.8(11.1)	1.59(1.16)	1.48 (1.04)	1.00(0.00)
0.9	66.5(67.9)	3.86(3.37)	125(140)	19.9(9.44)	1.54(1.07)	1.46 (1.09)	1.00(0.00)
1.0	62.0(67.3)	3.58(3.18)	124(142)	17.5(7.09)	1.45(1.01)	1.41 (0.92)	1.00(0.00)

Table 3: Average Detection Delays/ADDs(Standard Deviation of Detection Delays/STDs) for 1D data with $m = 20$

ϕ	TRAS	CMAB(s)	NAS	SASAM	CDSSD	CDSSD(I)	ORACLE
0.0	200(148)	200(184)	200(548)	200(133)	200(292)	200(355)	200(361)
0.1	157(96.3)	16.4(8.73)	161(460)	157(91.1)	6.43 (7.00)	8.36(11.6)	2.90(2.60)
0.2	115(63.0)	6.86(2.81)	151(415)	87.8(44.6)	2.21 (1.91)	2.94(1.89)	1.30(0.55)
0.3	93.2(50.1)	4.64(2.16)	125(371)	55.2(23.5)	1.45 (0.93)	1.45(0.99)	1.05(0.24)
0.4	78.3(42.5)	3.89(1.81)	111(344)	40.4(16.2)	1.23(0.69)	1.17 (0.55)	1.00(0.08)
0.5	68.1(37.4)	2.95(1.49)	107(323)	31.2(11.9)	1.16(0.61)	1.12 (0.49)	1.00(0.00)
0.6	60.4(36.6)	2.43(1.26)	93.0(299)	26.1(9.41)	1.15(0.63)	1.09 (0.42)	1.00(0.00)
0.7	54.1(38.0)	2.14(1.44)	76.1(259)	21.0(7.40)	1.14(0.49)	1.07 (0.42)	1.00(0.00)
0.8	47.6(31.3)	1.78(1.15)	87.3(289)	18.6(5.95)	1.11(0.45)	1.05 (0.30)	1.00(0.00)
0.9	44.6(27.4)	1.61(1.05)	87.8(292)	16.5(5.09)	1.09(0.38)	1.04 (0.28)	1.00(0.00)
1.0	41.3(27.8)	1.56(1.08)	75.8(253)	14.9(4.78)	1.09(0.45)	1.05 (0.32)	1.00(0.00)

Table 4: Average Detection Delays/ADDs(Standard Deviation of Detection Delays/STDs) for 1D data with $m = 30$

ϕ	TRAS	CMAB(s)	NAS	SASAM	CDSSD	CDSSD(I)	ORACLE
0.0	200(145)	200(180)	200(350)	200(134)	200(361)	200(444)	200(361)
0.1	158(97.8)	10.5(4.13)	163(295)	137(78.5)	2.90(2.60)	2.60 (3.11)	2.90(2.60)
0.2	114(52.0)	4.31(1.22)	123(228)	74.0(33.6)	1.30(0.55)	1.30 (0.67)	1.30(0.55)
0.3	90.1(36.3)	2.79(0.67)	86.6(180)	47.2(17.9)	1.05(0.24)	1.05 (0.23)	1.05(0.24)
0.4	74.5(27.60)	2.12(0.35)	81.9(170)	34.8(12.4)	1.00(0.08)	1.00 (0.08)	1.00(0.08)
0.5	63.9(23.1)	1.93(0.32)	73.5(157)	26.7(8.65)	1.00(0.00)	1.00 (0.03)	1.00(0.00)
0.6	55.5(20.4)	1.57(0.50)	62.2(138)	22.1(6.80)	1.00(0.00)	1.00 (0.00)	1.00(0.00)
0.7	50.0(16.1)	1.20(0.40)	62.3(144)	18.9(5.40)	1.00(0.00)	1.00 (0.00)	1.00(0.00)
0.8	45.2(0.33)	1.09(0.28)	61.7(138)	16.6(4.95)	1.00(0.00)	1.00 (0.00)	1.00(0.00)
0.9	41.0(12.5)	1.03(0.16)	58.9(137)	14.5(3.96)	1.00(0.00)	1.00 (0.00)	1.00(0.00)
1.0	38.6(11.9)	1.00(0.05)	59.3(147)	13.1(3.74)	1.00(0.00)	1.00 (0.00)	1.00(0.00)

Table 5: Average Detection Delays/ADDs(Standard Deviation of Detection Delays/STDs) for 2D data with $m = 20$

ϕ	TRAS	CMAB(s)	NAS	SASAM	CDSSD	CDSSD(I)	ORACLE
0.0	200(117)	200(172)	200(173)	200(166)	200(201)	200(203)	200(479)
0.1	197(107)	160(123)	203(181)	147(111)	87.6 (90.8)	159(188)	1.71(1.57)
0.2	164(85.1)	85.8(60.0)	193(176)	134(101)	24.4 (17.5)	61.2(79.2)	1.09(0.34)
0.3	138(70.0)	54.4(27.9)	202(187)	98.2(68.4)	15.9 (12.7)	22.9(28.4)	1.02(0.15)
0.4	119(65.8)	39.3(17.7)	184(176)	75.2(51.4)	12.9(10.7)	12.1 (11.3)	1.00(0.08)
0.5	105(60.1)	31.7(12.9)	192(174)	56.2(35.2)	11.2(9.96)	8.67 (7.74)	1.00(0.00)
0.6	96.2(60.0)	27.0(11.2)	187(182)	44.9(28.2)	10.2(9.94)	6.23 (5.27)	1.00(0.00)
0.7	89.7(56.5)	24.1(10.4)	201(188)	35.9(21.6)	9.45(8.93)	5.59 (4.77)	1.00(0.00)
0.8	79.2(53.0)	21.9(9.84)	191(185)	30.4(17.9)	9.02(9.26)	4.81 (4.33)	1.00(0.00)
0.9	75.6(53.5)	20.8(9.91)	196(188)	26.8(15.9)	8.22(9.24)	4.38 (3.70)	1.00(0.00)
1.0	74.1(54.2)	19.7(9.90)	192(177)	23.8(13.6)	7.47(8.07)	3.90 (3.54)	1.00(0.00)

Table 6: Average Detection Delays/ADDs(Standard Deviation of Detection Delays/STDs) for 2D data with $m = 40$

ϕ	TRAS	CMAB(s)	NAS	SASAM	CDSSD	CDSSD(I)	ORACLE
0.0	200(116)	200(171)	200(228)	200(161)	200(212)	200(285)	200(479)
0.1	193(107)	114(93.3)	208(240)	139(102)	31.9 (37.9)	145(156)	1.71(1.57)
0.2	152(72.0)	46.7(27.2)	195(233)	119(92.1)	10.5 (8.34)	36.2(51.4)	1.09(0.34)
0.3	125(59.5)	30.0(10.7)	187(212)	88.5(60.4)	6.68 (5.24)	12.6(11.8)	1.02(0.15)
0.4	104(51.0)	23.6(7.59)	204(236)	66.0(45.7)	5.33 (4.25)	6.47(5.75)	1.00(0.08)
0.5	91.8(47.9)	20.4(7.29)	188(225)	50.5(30.6)	4.74 (3.96)	4.74(3.55)	1.00(0.00)
0.6	81.6(44.7)	18.4(7.24)	179(210)	39.9(24.6)	4.00(3.54)	3.45 (2.74)	1.00(0.00)
0.7	73.8(42.0)	16.3(7.14)	177(196)	30.5(17.0)	3.64(3.33)	3.34 (2.59)	1.00(0.00)
0.8	66.1(40.8)	15.7(7.28)	196(210)	26.7(14.5)	3.12(2.83)	2.64 (1.81)	1.00(0.00)
0.9	59.8(37.4)	15.3(7.29)	181(203)	22.4(11.1)	2.95(2.86)	2.26 (1.66)	1.00(0.00)
1.0	56.3(37.5)	14.1(7.35)	185(190)	19.6(9.62)	2.89(3.00)	2.16 (1.54)	1.00(0.00)

Table 7: Average Detection Delays/ADDs(Standard Deviation of Detection Delays/STDs) for 2D data with $m = 60$

ϕ	TRAS	CMAB(s)	NAS	SASAM	CDSSD	CDSSD(I)	ORACLE
0.0	200(117)	200(180)	200(238)	200(172)	200(251)	211(291)	200(479)
0.1	184(101)	91.3(71.7)	188(234)	132(107)	20.3 (25.5)	102(131)	1.71(1.57)
0.2	151(77.3)	35.5(17.2)	196(244)	119(87.5)	6.24 (4.90)	24.4(29.1)	1.09(0.34)
0.3	118(53.7)	23.7(7.53)	187(241)	91.0(62.8)	4.29 (3.06)	7.43(7.45)	1.02(0.15)
0.4	95.9(44.9)	19.3(6.54)	168(203)	61.2(37.3)	3.39 (2.47)	4.62(3.45)	1.00(0.08)
0.5	83.3(38.9)	16.8(6.12)	199(246)	45.2(26.1)	2.82 (2.05)	2.96(2.14)	1.00(0.00)
0.6	72.5(34.9)	14.8(6.11)	191(251)	35.3(19.2)	2.57(2.32)	2.48 (1.78)	1.00(0.00)
0.7	66.8(33.7)	13.7(6.14)	190(243)	28.5(15.0)	2.21 (1.58)	2.27(1.53)	1.00(0.00)
0.8	60.5(32.2)	12.7(6.18)	178(232)	24.2(11.9)	1.92(1.35)	1.90 (1.41)	1.00(0.00)
0.9	54.2(28.9)	12.1(6.21)	168(213)	21.4(10.4)	1.91(1.43)	1.64 (0.98)	1.00(0.00)
1.0	50.1(28.9)	11.9(6.12)	168(217)	18.9(9.26)	1.90(1.48)	1.54 (1.01)	1.00(0.00)